The HUSH-SETDB1-MORC2 epigenetic repressor complex restricts herpesvirus infection in association with PML nuclear bodies

Simon Roubille, Franceline Juillard, Tristan Escure, Olivier Binda, Armelle Corpet, Stuart Bloor, Camille Cohen, Pascale Texier, Noémie Oziol, Oscar Haigh, et al.

The HUSH-SETDB1-MORC2 epigenetic repressor complex restricts herpesvirus infection in association with PML nuclear bodies

Simon Roubille
University Claude Bernard Lyon 1
Franceline Juillard
University Claude Bernard Lyon 1
Tristan Escure
University Claude Bernard Lyon 1
Olivier Binda
University Claude Bernard Lyon 1, University of Ottawa
Armelle Corpet
University Claude Bernard Lyon 1
Stuart Bloor
University of Cambridge
Camille Cohen
Université Montpellier, UMR 5235, LPHI Laboratory of Pathogen Host Interactions
Pascale Texier
Université Claude Bernard Lyon 1
Noémie Oziol
CEA, Center for Immunology of Viral, Auto-immune, Hematological and Bacterial diseases
Oscar Haigh
CEA, Center for Immunology of Viral, Auto-immune, Hematological and Bacterial diseases
Olivier Pascual
Université Claude Bernard Lyon 1
Yonatan Ganor
Université Paris Cité, Institut Cochin
Frédérique Magdinier
Aix-Marseille Univ., INSERM, Marseille Medical Genetics
Marc Labetoulle
CEA, Center for Immunology of Viral, Auto-immune, Hematological and Bacterial diseases
Paul Lehner
University of Cambridge https://orcid.org/0000-0001-9383-1054
Patrick Lomonte (✉ patrick.lomonte@univ-lyon1.fr)

CNRS, University Claude Bernard Lyon 1 https://orcid.org/0000-0001-9248-648X

Letter

Keywords:

Posted Date: February 7th, 2023

DOI: https://doi.org/10.21203/rs.3.rs-2521252/v1

Additional Declarations: There is **NO** Competing Interest.

The HUSH-SETDB1-MORC2 epigenetic repressor complex restricts herpesvirus infection in association with PML nuclear bodies

Simon Roubille[1,#], Franceline Juillard[1,#], Tristan Escure[1], Olivier Binda[1,2], Armelle Corpet[1], Stuart Bloor[3], Camille Cohen[1,4], Pascale Texier[1], Noémie Oziol[8], Oscar Haigh[8], Olivier Pascual[5], Yonatan Ganor[6], Frédérique Magdinier[7], Marc Labetoulle[8,9], Paul J. Lehner[3], and Patrick Lomonte[1,*]

1. Univ Lyon, Université Claude Bernard Lyon 1, CNRS UMR 5261, INSERM U1315, LabEx DEV2CAN, Institut NeuroMyoGène-Pathophysiology and Genetics of Neuron and Muscle (INMG-PGNM), team Chromatin dynamics, Nuclear Domains, Virus. F-69008, Lyon, France
2. University of Ottawa, Faculty of Medicine, Department of Cellular and Molecular Medicine, K1H 8M5, Ottawa, Ontario, CANADA
3. Cambridge Institute of Therapeutic Immunology and Infectious Disease, Jeffrey Cheah Biomedical Centre, Cambridge Biomedical Campus, Cambridge, CB2 OAW, U.K.
4. Université Montpellier, UMR 5235, LPHI Laboratory of Pathogen Host Interactions, team "GATAC-Malaria". F-34095, Montpellier, France.
5. Univ Lyon, Université Claude Bernard Lyon 1, CNRS UMR 5284, INSERM U1314, Institut NeuroMyoGène-Mechanisms in Integrated Life Sciences (INMG-MeLiS), Team "Synaptopathies et Autoanticorps", F-69008, Lyon, France.
6. Université Paris Cité, Institut Cochin, INSERM U1016, CNRS UMR 8104, 75014, Paris, France
7. Aix-Marseille Univ., INSERM, Marseille Medical Genetics (MMG), Marseille, France
8. Center for Immunology of Viral, Auto-immune, Hematological and Bacterial diseases (IMVA-HB). Commissariat à l'Énergie Atomique et aux Énergies renouvelables, Université Paris-Saclay, INSERM U1184, Fontenay-aux-Roses & Le Kremlin-Bicêtre, France.
9. Service d'Ophtalmologie, Hôpital Bicêtre, Université Paris-Saclay, APHP, CRMR OPHTARA, Le Kremlin-Bicêtre, France.

# contributed equally

* corresponding author : patrick.lomonte@univ-lyon1.fr

Abstract :

The establishment of latent herpes simplex virus 1 (HSV-1) infection is controlled by promyelocytic leukemia nuclear bodies (PML NBs). Viral genomes are recruited to PML NBs structures and chromatinized by repressive H3.3K9me3 modified H3.3 histone variant to form viral DNA-containing PML-NBs (vDCP NBs). Exactly how this occurs is unclear. Here we identify an essential role for the HUSH complex and its SETDB1 and MORC2 effectors in the establishment and maintenance of latent herpes simplex virus 1 (HSV-1) infection. We show that the formation of repressive heterochromatin is dependent on HUSH, SETDB1 and MORC2 in vDCP NBs, and depletion of any of these components prior to viral infection decreases H3K9me3 levels over latent/quiescent HSV-1 genomes. Once latency is established, depletion of HUSH, SETDB1, or MORC2 by shRNAs or the HIV-2 Vpx protein, induces the reactivation of HSV-1 in infected primary human fibroblasts as well as human induced pluripotent stem cell-derived sensory neurons (hiPSDN). Our data demonstrate the potent antiviral restriction activity of the HUSH/SETDB1/ MORC2 complex to a non-integrated human herpesvirus, its close association with PML NBs, and introduces a new target for anti-herpesvirus therapy.

Introduction

The establishment of latent herpes simplex virus 1 (HSV-1) infection involves a complex interplay of cellular and molecular events. At the epigenetic level, this requires the viral chromatinization and interaction of latent episomal viral genomes with their nuclear environment [1,2]. Promyelocytic leukemia nuclear bodies (PML NBs also named ND10) are nuclear membrane-less organelles involved in the transcriptional control of HSV-1 latent genomes [3,4]. The protein composition of PML NBs is highly dynamic due to their phase separation properties [5]. Following HSV-1 nuclear entry, PML NBs sequester HSV-1 genomes [3,6,7] and control the acquisition of repressive histone marks of PML NBs-associated HSV-1 genomes (also named viral DNA-containing PML NBs, vDCP NBs or ND10-like) [8]. VDCP NBs, a major hallmark of HSV-1 latently infected neurons, are characterized by their ability to maintain latent HSV-1 genomes in a transcriptionally inactive, but reversible, state of quiescence [3,4]. PML NBs, and by extension vDCP NBs, are disrupted by ICP0, a virus-encoded ubiquitin E3 ligase, which counteracts the intrinsic host antiviral defense mechanisms, and is essential for the initiation of HSV-1 lytic reactivation and replication from latency [8–12]. Di- and trimethylation of lysine 9 of histone H3 (H3K9me3) marks repressive heterochromatin in general and repressed latent HSV-1 genomes in particular [8,13], but the cellular factor(s) involved in the establishment and maintenance of HSV-1 latency remain unknown.

Three methyltransferases are responsible for the deposition of H3K9me3 in mammalian cells: SUV39H1, SUV39H2 and ESET/SETDB1 (hereafter named SETDB1) [14–16]. In mouse cells SETDB1 is a major constituent of PML NBs [17]. SETDB1 is responsible for silencing proviral elements in ESC cells [18] and for the establishment and maintenance of human cytomegalovirus latency in CD34+ cells [19]. We identified HUSH (Human Silencing Hub) as an epigenetic repressor complex which silences integrated retroelements [20,21]. These include retroviruses, such as latent HIV [20], as well as retrotransposons [22–26]. HUSH also silences non-integrated viruses, including murine leukemia virus (MLV) (Zhu *et al*, 2018) and adeno-associated virus (AAV) [27]. HUSH is made up of three core components, TASOR (transgene activation suppressor), MPP8 (M-phase phosphoprotein 8) and Periphilin and recruits two effector proteins: the SETDB1 methyltransferase deposits repressive H3K9me3 heterochromatin [20], and the MORC2 (microrchidia CW-type zinc-finger) ATP-dependent

chromatin remodeler compacts heterochromatin [28,29], and is frequently mutated in Charcot-Marie-Tooth disease CMT2Z patients [28–32].

Here we investigate the role of SETDB1 and the HUSH complex in the regulation of latent HSV-1, an unintegrated herpesvirus genome. We find that HUSH, SETDB1 and MORC2 together with PML NBs create an epigenetic environment which allows the establishment and maintenance of HSV-1 latency in primary human fibroblasts as well as sensory neurons derived from human induced pluripotent stem cells (hiPSDN), the physiological site of HSV-1 latency.

Results

SETDB1 is a major determinant of vDCP NBs. To understand how the HSV-1 viral genome is maintained in the latent state we initially infected primary human fibroblast cells (hFC) with a latency/quiescence-prone HSV-1 (lqHSV-1) mutant [8], a model system we previously showed to reproduce the formation of vDCP NBs, as seen in trigeminal neurons of latently infected mice and human [3,4]. Proteins of the HIRA H3.3 histone chaperone complex, HIRA and UBN1 bind naked non-chromatinised DNA [33] and are recruited to vDCP NBs where they bind incoming HSV-1 genome [8]. LqHSV-1 genome chromatinization with H3.3 by the HIRA complex and PML protein results in K9 trimethylation of the H3.3 histone variant [8].

UBN1 co-precipitates with a histone H3K9 methyltransferase activity [34], and SETDB1 is a component of PML NBs in mouse cells [17]. Therefore, we investigated whether SETDB1 plays a role in HSV-1 dependent silencing. SETDB1 was readily detected in PML NBs of non-infected (NI) and infected hFC (**Supplementary Fig. 1a**), remaining associated with PML NBs in lqHSV-1 infected cells for at least 7 days post-infection (dpi) (**Supplementary Fig. 1a**) and co-localizing with lqHSV-1 genomes in all infected cells (**Supplementary Fig. 1b**). These data suggest SETDB1 and its partner proteins are putative molecular determinants of latent/quiescent HSV-1 epigenetic regulation.

The HUSH complex and MORC2 accumulate in vDCP NBs following HSV-1 PML NBs-associated latent infection. Given the close functional interaction between SETDB1, the HUSH complex and MORC2, we investigated their presence in PML NBs and vDCP NBs in NI and infected cells. All proteins detected by IF-FISH, including endogenous SETDB1 and MPP8, were associated with vDCP NBs in latently infected hFC (**Fig. 1 a-e, and Supplementary Fig. 2**

for tagged MPP8) and were present in the same structures as exemplified by the concomitant detection of SETDB1 and MPP8 co-localizing with viral genomes (**Fig. 1c**). Unlike endogenous SETDB1 and over-expressed proteins, none of the endogenous core HUSH complex proteins or MORC2 showed PML NBs localization in NI hFC (**Supplementary Fig. 3 and Supplementary Fig. 4**). We performed ChIP analysis to determine whether the HUSH complex and its effector proteins were recruited to the HSV-1 viral genome. Multiple loci (promoter and/or coding region, see MM for details) within the viral genome were analyzed, which together represent all classes of lytic and latent genes (**Fig. 2a**). Only antibodies against endogenous MPP8 and, to a lesser extent, MORC2, gave reliable results by ChIP, and showed a strong interaction between MPP8 and all viral loci (**Fig. 2b-c and Supplementary Fig. 5** for complete set of viral genes for MORC2). Ectopic tagged HUSH components, including MPP8 and MORC2, were also enriched on the latent viral genome (**Fig. 2d, and expanded data** including significances in **Supplementary Fig. 6**). Together, these data suggest a role for the HUSH complex, together with SETDB1 and MORC2, in the epigenetic regulation of latent HSV-1.

The HUSH complex with SETDB1 and MORC2 control repressive histone marks on latent PML NBs-associated HSV-1 genome. To further investigate the role of HUSH components in the acquisition of the H3K9me3 mark on the lqHSV-1 genome, we took a knock down approach, transducing hFC with previously validated and specific shRNAs [20,28] (**Fig 3a**) and verified their efficiency at the protein level (**Fig. 3b-f**).Depletion of any one of the five proteins induced a significant decrease of the H3K9me3 mark across the latent viral genome, though this was less pronounced following TASOR depletion (**Fig. 3g and expanded data including significances in Supplementary Fig. 7**). A siRNA targeting SETDB1 gave similar results (**Supplementary Fig. 8**). The HIV-2 and SIV Vpx accessory protein degrades TASOR and destabilizes the HUSH complex [24,38]. HIV-2 Vpx expression induced TASOR degradation (**Fig. 3h**), and reduced the H3K9me3 mark over the lqHSV-1 genome (**Fig. 3i**). These data establish the HUSH complex together with SETDB1 and MORC2 as a major pathway in the acquisition of the repressive chromatin H3K9me3 mark on the latent HSV-1 genome.

HUSH-SETDB1-MORC2 entity maintains PML NBs-associated HSV-1 latency. LqHSV-1 is thermosensitive and acquires its latency/quiescent state at 38.5°C in hFC, leading to the

formation of vDCP NBs and transcriptionally silent viral genomes. Latency can be reversed by destabilizing vDCP NBs with the HSV-1 protein ICP0 and reverting the temperature to 32°C [8]. To determine if the HUSH complex is required to maintain lqHSV-1 silencing, individual components of the HUSH-SETDB1-MORC2 complex were depleted after the acquisition of latency and formation of the vDCP NBs (**Fig. 4a**). Inducible shRNA-mediated depletion (**Supplementary Fig. 9a-h**) of any HUSH complex component led to transcriptional activation of the lqHSV-1, as determined by the appearance of viral lytic gene-encoding mRNAs (**Fig. 4b-f**). Furthermore, viral replication compartments (RC), a marker of progressive viral lytic infection, were readily detected in cells from monolayers showing evidence of reactivation (**Fig. 4g**). Viral plaque formation was also observed on hFC monolayers following HUSH depletion but not in the control (shCTRL) (**Supplementary Fig. 9g**). To confirm that inactivation of the HUSH complex induced production of infectious viral progeny, supernatants from the hFC monolayers were titrated on human bone osteosarcoma (U2OS) epithelial cells (**Fig. 4h**). Supernatants from HUSH-depleted, but not shCTRL components induced viral plaque formation (**Fig. 4h**, supernatants of shCTRL and shMORC2 (shown as an example) and **Fig. 4i** for quantitation). Degradation of HUSH by HIV-2 Vpx also induced transcriptional reactivation, appearance of RCs, and viral plaques (**Fig. 5a-d**) and production of infectious virus in Vpx-expressing cells (**Fig. 5e-f**). These data demonstrate that the HUSH epigenetic repressor complex together with SETDB1 and MORC2 are required for stabilization of HSV-1 PML NB-associated latency.

The HUSH complex with SETDB1 and MORC2 maintain HSV-1 latency in human neurons.

The hFC infection model provides a practical system to characterize essential epigenetic features controlling PML NB-associated HSV-1 latency. As sensory neurons of the trigeminal ganglia (TG) are the predominant sites of latent HSV-1 infection, it was essential to determine whether HUSH is also able to restrict latent HSV-1 infection in these cells. We therefore established latent HSV-1 infection in human sensory neurons derived from human induced pluripotent stem cells (hiPSDN) **(Supplementary Fig. 10a)**. These neurons recapitulate the molecular, electrophysiological, and biochemical features of sensory neurons in general, and nociceptive neurons in particular **(Supplementary Fig. 10b-g)**. hiPSDN contain PML NBs (**Supplementary Fig. 10h**), as seen in murine and human TG neurons [3,4]. To confirm the validity of the hiPSDN infection model, we infected hiPSDN with

the lqHSV-1 virus and measured reactivation following expression of the ICP0 viral protein or its inactive RING Finger domain mutant (ICP0RFmut) (**Fig. 6a**). ICP0, but not its RF mutant, destabilizes the PML NBs and vDCP NBs [8,9] and induced transcriptional reactivation of lqHSV-1 (**Fig. 6b**), resulting in production of infectious viral progeny (**Fig. 6c-d**). Immunofluorescent detection of the ICP4 and NF200 proteins further confirmed the presence of RCs in reactivating neurons (**Fig. 6e**). Finally, shRNA-mediated MORC2 depletion from lqHSV-1-infected hiPSDNs (**Fig. 7a, and Supplementary Fig. 11**) also induced the transcriptional reactivation of lqHSV-1, as determined by the temporal increase in lytic viral mRNAs (**Fig. 7b**), confirming a role for the HUSH complex in the transcriptional silencing of PML NBs-associated latent HSV-1. Furthermore, infectious progeny were released from reactivating neurons, as supernatants from day 7 shMORC2-treated neurons induced viral plaques in U2OS cells (**Fig. 7c-d**). Taken together, these data demonstrate the essential role of MORC2, and by extension the HUSH complex, in maintaining HSV-1 latency in neurons. The HUSH complex, SETDB1 and MORC2, together with PML NBs therefore represent a major nuclear restriction pathway controlling HSV-1 latency.

Discussion

The neurotropic nature of HSV-1 and its ability to spread from the peripheral to the central nervous system makes it an important etiological candidate for non-genetic infection-associated neurodegenerative pathologies [39,40]. It is therefore important to understand the mechanisms that trigger HSV-1 to induce and maintain the latent state. The formation of repressive heterochromatin through K9me3 modification of histone H3.1 and/or histone variant H3.3 and chromatin compaction is an important mechanism for transcriptional silencing of endogenous retrotransposons and human immunodeficiency virus as well as HSV-1 genomes, leading to the establishment of a latent/quiescent state [8,13,18,20,21,41,42]. Epigenetic regulation associated with viral chromatinization is therefore a hallmark of latent HSV-1. The HUSH-SETDB1-MORC2 repression complex is well described for its essential role in maintaining integrated retroelements in an inactive state [20,28]. MPP8 and SETDB1 interact and cooperate in the silencing of satellite DNA repeats in mouse embryonic stem cells [26]. The HUSH complex, together with NP220/ZNF638 also silence non-integrated murine leukemia virus [25]. Similarly, NP220 and HUSH silence recombinant AAV (rAAV) vectors in a serotype-

dependent manner [27]. However, the actual contribution of HUSH in maintaining latency of a genuine unintegrated episomal virus such as HSV-1 has not been determined.

We and others have demonstrated the heterogeneity of HSV-1 latency in neurons *in vivo* in mouse models. This heterogeneity exists at least at the level of viral genome chromatin marks acquisition and interaction of latent viral genomes with the nuclear environment. The latter is exemplified by the encapsulation of the viral genomes within PML NBs, and referred as to vDCP NBs [3,4,13,49,50]. In the present study, we decipher a mechanism of establishment and maintenance of PML NBs-associated latent HSV-1 genomes involving the apposition of the H3K9me3 mark on the viral chromatin by the HUSH-SETDB1-MORC2 repression complex. We show that his pathway is closely associated with the formation of vDCP NBs. The HUSH-SETDB1-MORC2 complex is essential for the acquisition of the H3K9me3 chromatin mark on latent HSV-1 genomes and for their transcriptional repression. A functional HUSH-SETDB1-MORC2 complex is also essential for maintaining PML NBs-associated HSV-1 latency in neuronal cells, as suggested by the importance of MORC2 in the control of the stability of HSV-1 latency in hiPSDN. Given the essential role of MORC2 for the HUSH complex activity [28,43], this suggests that the HUSH-SETDB1-MORC2 repression complex acts as a major epigenetic regulatory entity to maintain HSV-1 latency in neurons. SETDB1 is known for its major involvement in neurons survival and brain development [44], and the role of HUSH-MORC2 in developmental aspects of the CNS has recently been put to the limelight [45]. The involvement of the HUSH-SETDB1-MORC2 entity in the acute control, then long-term maintenance, of the latency of a neurotropic virus is thus of particular interest.

The association of the HUSH-SETDB1-MORC2 entity with vDCP NBs most likely links its epigenetic activity with the stability of the vDCP NBs. The HSV-1 ICP0 protein destabilizes PML NBs [46] and vDCP NBs [8], and has been shown to erase the H3K9me3 mark on viral chromatin upon HSV-1 lytic cycle and establishment/maintenance of latency [47,48]. We show that ICP0 is able to induce HSV-1 reactivation in latently infected iPSDN. This suggests a direct and/or indirect impact of ICP0 on the HUSH-SETDB1-MORC2 repression complex activity by destabilizing vDCP NBs.

The HUSH-SETDB1-MORC2 entity acting as a novel nuclear restriction pathway in concert with the activity of PML NBs, extends at the epigenetic level the intrinsic response of the cell for the control of the infection by a neurotropic virus (**Fig. 7d**). This pathway is a direct target of the activity of the viral protein ICP0, likely through the destabilization of

vDCP NBs, to promote reactivation of HSV-1. Stabilizing this important pathway would enable the control of neuronal damage caused by the spread of the virus in the nervous system following reactivation. Alternatively, destabilizing the HUSH-SETDB1-MORC2 entity might be considered as a complementary approach to proposed therapies designed to modify viral genomes to prevent their reactivation. As an example, viral genomes editing using meganucleases or CRISPR/Cas9 technologies has been proposed to eliminate latent HSV reservoirs [52–55]. Provoking sub-reactivation of HSV-1 by inactivating the HUSH-SETDB1-MORC2 entity could then potentiate the use of these technologies, provided that it does not induce global epigenetic modifications that would put a threat on cellular defense mechanisms. On a different aspect, targeting HUSH for degradation has been discussed as part of a "shock and kill" strategy in HIV cure designed to eliminate reservoir cells responsible for rebounds when antiretroviral treatments are stopped [56]. Our study establishes HUSH as an essential actor for the maintenance of HSV-1 latency. Targeting HUSH degradation, moreover in immunocompromised patients, without controlling herpesvirus lytic cycle, e.g. by administration of anti-herpesviral drugs, could therefore compromise the integrity of patients. Indeed, this could lead to uncontrolled HSV-1 spread in the PNS and CNS potentially responsible for neuronal and/or ocular pathologies as a result of herpesvirus reactivation. In that context, the "block and lock" strategy to create a "deep latency" of HIV seems indeed more appropriate considering the likely broad involvement of the HUSH-SETDB1-MORC2 entity in the control of multiple latent viruses. Finally, the importance of the HUSH-SETDB1-MORC2 repression complex together with PML NBs to control a genuine unintegrated virus, such as HSV-1, could be broaden to other viruses remaining latent/quiescent as episomes in the nucleus of infected cells.

Methods

Virus strains

The HSV-1 mutant *in*1374 is derived from the 17 *syn* + strain and expresses a temperature-sensitive variant of the major viral transcriptional activator ICP4 [57]. *In*1374 is derived from *in*1312, a virus derived from the VP16 insertion mutant *in*1814 [58], which additionally carries a deletion/frameshift mutation in the ICP0 open reading frame [59] and contains an HCMV-*lacZ* reporter cassette inserted into the UL43 gene of *in*1312 [60]. This virus has been used and described previously [4,6]. *In*1374 was grown and titrated at 32°C in the presence of 3 mM HMBA [61]. For simplicity, *in*1374 will be renamed lqHSV-1 (for latent/quiescent HSV-1).

Cells

Human BJ primary foreskin fibroblasts (ATCC, CRL-2522), human embryonic kidney (HEK 293T, ATCC CRL-3216, kind gift from M. Stucki, University Hospital Zürich) cells, human bone osteosarcoma (U2OS) epithelial cells (kind gift from R. Everett), and baby hamster kidney (BHK-21) cells (kind gift from R. Everett) cells were grown in Dulbecco's Modified Eagle's Medium (DMEM) (Sigma-Aldrich, D6429) supplemented with 10% fetal bovine serum (Sigma, F7524), L-glutamine (1% v/v), 10 U/mL penicillin, and 100 mg/mL streptomycin (Sigma- Aldrich, P4458). BJ cell division is stopped by contact inhibition. Therefore, to limit their division, cells were seeded at confluence before being infected at a multiplicity of infection (m.o.i.) of 3, and then maintained in 2% serum throughout the experiment.

Human induced pluripotent stem (hiPS) cells (clone AG08C5) were derived at the Marseille Medical Genetics (MMG) [62], were maintained in culture on plates coated with Matrigel (Corning, 354277) in mTeSR+ (Stemcell Technologies, 05825). The medium was changed every 2 days. Cells were passaged using tryple (Gibco, 354277), washed, and replated at 2.10e5 cells. Revitacell (Rock inhibitor) was added during the passage in order to promote cell survival.

All cells were tested negative for mycoplasma.

Generation of sensory neurons

Differentiation of hiPSC into sensory neurons was performed according to [63]. Briefly, hiPSC colonies at 60% confluence were dissociated using tryple and pelleted at 800 rpm for 4 minutes (room temperature). To generate sensory neurons, the cells were maintained on Matrigel-coated plates in DMEM/F12 with defined supplements. Cultures were supplemented from day 1 to day 10 with 10% KSR, 1% penicillin/streptomycin, 0.3 mM LDN-193189, 2 mM A83-01, 6 mM CHIR99021, 2 mM RO4929097, and 3 mM SU5402. Retinoic acid 0.3 mM was included in all cultures. The medium was refreshed every 2 days. The mitotic inhibitors fluorodeoxyuridine was added at day 6 until day 10. The medium was then replaced with fresh medium without fluorodeoxyuridine. Once day 10 is reached, cultures were maintained in neurobasal medium supplemented with 10 ng/ml neurotrophin 3 (NT3), 20 ng/ml NGF with half of the medium refreshed every other day for up to 2 weeks.

Nociceptive properties of hiPSDN

Sensory neurons with nociceptive activity are characterized by their ability to release calcitonin gene-related peptide (CGRP) following capsaicin treatment. Neurons were treated overnight with either 1, 10, 100uM of Capsaicin or KCl. Supernatants were then speedvac and analyzed by « alpha-CGRP human enzyme immunoassay » (Cat. No. S-1199 from Peninsula Laboratories,San Carlos, CA, USA). All was performed according to the manufacturer instructions. Analysis of the results was performed with Prism software, by applying the "log (inhibitor) vs. response -- Variable slope (four parameters)" model.

Reagents

Drugs and molecules used for cell treatments are described below (duration is mentioned in the main text).

Name	Supplier/Catalog code-number	Final concentration
Retinoic acid	Stemcell (#72262)	0,3mM
A83-01	Stemcell (#72024)	2mM
blasticidin	Invivogen, ant-bl	5ug/ml
CHIR99021	Stemcell (#72054)	6mM
doxycycline	Sigma-Aldrich (#D9891)	1ug/ml
5-Fluoro-2'-deoxyuridine	Merck (#343333)	40uM
hygromycin	Thermo Fisher Scientific (#10687010)	250ug/ml
LDN193189	Stemcell (#72147)	0,3mM
NGF	SIGMA (#H9666-10µg)	20ng/ml
NT3	Miltenyi Biotec (#130-096-287)	10ng/ml
Polybrene	Merck (#TR-1003)	8ug/ml
Protamine	Sigma-Aldrich (#P4020-100G)	8ug/ml
Puromycin	Invivogen, ant-pr	1ug/ml
revitacell	Thermo Fisher Scientific (#A2644501)	1X (dilution by 100)
RO4929097	Clinisciences (#A4005-10mg)	2mM
SU5402	Stemcell (#73914)	3mM

Electrophysiology

Whole-cell patch-clamp recordings were performed at 30 °C using a Multiclamp 700B amplifier. Electrodes had a tip resistance of 5–7 Mohm when filled with intracellular solution (140mM CsCl, 1mM MgCl2, 1mM CaCl2, 10mM EGTA, 1mM BAPTA, 10mM HEPES and 4mM MgATP). The perfusion medium contained 145mM NaCl, 2.4mM KCl, 10mM HEPES, 10mM D-glucose, 2mM CaCl2 and 2mM MgCl2, and was supplemented when necessary with 1 µM TTX, to test the presence of voltage gated sodium channels. Recordings were filtered at 2–5 kHz and acquired at 5–10 kHz. Currents were recorded in voltage clamp mode at a holding potential of -80 mV. 250 ms and 10 mV, incremental steps were preformed to test the current-voltage relationship and elicit voltage gated sodium channels opening. Cells in which the access resistance changed by 20% during the recording or exceeded 20 Mohm were discarded. Data were acquired and analyzed with clampex 10 software (Axon).

Lentivirus production and establishment of cell lines

BJ or hiPSDN cells stably expressing transgenes or shRNA were obtained by lentiviral transduction. Briefly, plasmids of interest (see plasmids section) were co-transfected with psPAX.2 (Addgene #12260) and pMD2.G (Addgene #12259) plasmids with a ratio of 3:2:1 by the calcium phosphate method into HEK 293T cells to package lentiviral particles. After 48 h, supernatant containing replication-incompetent lentiviruses was filtered and applied for 24 h on the target cells in a medium containing polybrene 8 µg/mL (Sigma) [64] in the case of BJ cells or protamine 8ug/ml (Sigma) in the case of hiPSDN . Stable transfectants were selected with Blasticidin S (5 µg/mL, Invivogen), puromycin (1 µg/mL, Invivogen), or hygromycin (250 ug/mL, thermo), and a polyclonal population of cells was used for all experiments

Plasmids

Lentivirals plasmids for shRNA		
Plasmids	**Constructions**	**Target sequences**
pLKO-shCTRL	shCTRL was cloned through AgeI, EcoRI digestion into pLKO.1 hygro (Addgene 24150)	CCTAAGGTTAAGTCGCCCTCG
pLKO-shSETDB1	shSETDB1 was cloned through AgeI, EcoRI digestion into pLKO.1 hygro (Addgene 24150)	ATCCCTCCCATCCCATATTTG
pHR-SIREN-shTASOR	shTASOR was cloned through BamHI-EcoRI digestion	GAGGAAGCTTGAGGATCTA
pHR-SIREN-shMPP8	shMPP8 was cloned through BamHI-EcoRI digestion	AAGAAGACCCCGAGAAAGG
pHR-SIREN-shPPHLN	shPPHLN was cloned through BamHI-EcoRI digestion	AGCTAACCACTCGCTCTAA
pHR-SIREN-shMORC2	shMORC2 was cloned through BamHI-EcoRI digestion	GCGGAACATTGGTGATCAT
Lentivirals plasmids for inducible shRNA		
pLKO-tet-ON-shCTRL	shCTRL was cloned through AgeI, EcoRI digestion into pLKO-tet-on-puro (Addgene 21915)	CCTAAGGTTAAGTCGCCCTCG
pLKO-tet-ON-shSETDB1	shSETDB1 was cloned through AgeI, EcoRI digestion into pLKO-tet-on-puro (Addgene 21915)	ATCCCTCCCATCCCATATTTG
pLKO-tet-ON-shTASOR	shTASOR was cloned through AgeI, EcoRI digestion into pLKO-tet-on-puro (Addgene 21915)	GAGGAAGCTTGAGGATCTA
pLKO-tet-ON-shMPP8	shMPP8 was cloned through AgeI, EcoRI digestion into pLKO-tet-on-puro (Addgene 21915)	AAGAAGACCCCGAGAAAGG
pLKO-tet-ON-shPPHLN	shPPHLN was cloned through AgeI, EcoRI digestion into pLKO-tet-on-puro (Addgene 21915)	AGCTAACCACTCGCTCTAA
pLKO-tet-ON-shMORC2	shMORC2 was cloned through AgeI, EcoRI digestion into pLKO-tet-on-puro (Addgene 21915)	GCGGAACATTGGTGATCAT

Lentivirals plasmids for transgene expression		
Plasmids	**Constructions**	**Cloning**
pSFFV-FLAG-MPP8-WPRE-pPGK-BlastoR	Express FLAG-MPP8	[20]
pSFFV-V5-Periphilin-WPRE-pPGK-HygroR	Express V5-PPHLN	[20]
pSFFV-V5-NLS-MORC2-WPRE-pPGK-HygroR	Express V5-MORC2	[20]
pSFFV-HA-TASOR-pPGK-Puro	Express HA-TASOR	[28]
pHRSIN-RSV-3*HA-HIV-2 Vpx	Express HA-Vpx (HIV2 strain)	[65]
pLVX-3*HA-HIV-2 Vpx	Express HA-Vpx (HIV-2 strain) in a doxycycline inducible manner	Amplify by PCR from pHRSIN-RSV-3*HA-HIV-2 Vpx and cloned into pLVX (Takara) through AgeI, BamHI digestion
pLentiN-HA-SETDB1	Express HA-SETDB1	Amplify by PCR from pCMV2-FLAG-SETDB1 (Kind gift from Dr Slimane Ait-Si-Ali) and cloned into pLentiN through AscI, BstBI digestion
pLKO.DCMV.TetO.cICP0	Express ICP0	Kind gift from Dr Roger Everett [66]
pLKO.DCMV.TetO.cICP0ΔRF	Expressed ICP0ΔRF unable to degrade PML	Kind gift from Dr Roger Everett [66]
pcDNA3-HIRA-myc	Express HIRA-myc	subcloned into pcDNA3 through EcoRI-XhoI digestion
pcDNA3-myc-UBN1	Express myc-UBN1	subcloned into pcDNA3 through BamH1-EcoRV digestion
pcDNA3-3*HA-SETDB1	Express 3*HA-SETDB1	[67]

Immunofluorescence

Cells were seeded on either 24-well plate containing one coverslip or directly into 8-wells labteck. Cells were fixed for 10 min with 4% paraformaldehyde, washed three times with PBS, then permeabilized for 5 min in a PBS solution containing 0.5% Triton X-100. Primary antibodies were diluted in PBS containing 3% newborn goat serum (see antibodies section). After incubation at room temperature for 1 h, coverslips were washed at least three

times with PBS plus 3% newborn goat serum, and then incubated with goat anti-mouse or anti-rabbit (H+L) cross-absorbed secondary antibodies Alexa-488, Alexa-555 or Alexa-647 (Invitrogen). After a further 30-min incubation, coverslips were washed three times with PBS plus 3% newborn goat serum. Following immunostaining, nuclei were stained with DAPI (Invitrogen Life Technologies, D1306) diluted in PBS at 0,1µg/mL for 5 minutes at RT°C. Coverslips were mounted in Fluoromount-G (SouthernBiotech, 0100-01) and stored at 4°C before observation.

DNA-FISH and immuno-FISH

HSV-1 DNA FISH probes consisting of cosmids 14, 28 and 56 [68] comprising a total of ~90 kb of the HSV-1 genome were labeled by nick-translation (Invitrogen) with dCTP-Cy3 (GE Healthcare) and stored in 100% formamide (Sigma). The DNA-FISH and immuno-DNA FISH procedures have been described previously [3,69]. Briefly, infected cells were fixed in 2% PFA. Infected cells were then permeabilized in 0.5% Triton X-100. Heat-based unmasking was performed in 100 mM citrate buffer, and sections were post-fixed using a standard methanol/acetic acid procedure and dried for 10 min at RT. DNA denaturation of the section and probe was performed for 5 min at 80°C, and hybridization was carried out overnight at 37°C. Sections were washed 3 x 10 min in 2 x SSC and for 3 x 10 min in 0.2 x SSC at 37°C, and nuclei were stained with Hoechst 33258 (Invitrogen). All sections were mounted under coverslips using Fluoromount-G (SouthernBiotech, 0100-01)

For immuno-DNA FISH, cells were treated as described for DNA-FISH up to SSC washing. Cells were then treated with PBS-Normal Goat Serum to saturate non-specific site for 1h at RT. Cells were then incubated with the primary antibody 1h (see antibodies section). After three washes, secondary antibody was applied for 1 h. Following immunostaining, nuclei were stained with DAPI (Invitrogen Life Technologies, D1306) diluted in PBS at 0,1µg/mL for 5 minutes at RT°C. Coverslips were mounted in Fluoromount-G (SouthernBiotech, 0100-01) and stored at 4°C before observation.

Microscopy, imaging, and quantification

Images were acquired with the Axio Observer Z1 inverted wide-field epifluorescence microscope (100X or 63X objectives/N.A. 1.46 or 1.4) (Zeiss) and a CoolSnap HQ2 camera from Photometrics. Identical settings and contrast were applied for all images of the same experiment to allow data comparison through ImageJ.

ChIP and quantitative PCR

Cells were fixed with methanol-free formaldehyde (#28908, Thermo Fisher Scientific) 1% for 5 min at RT, and then glycine 125 mM was added to arrest fixation for 5 min. After two washes with ice-cold PBS, the cells were scraped and resuspended in “Lysis Buffer” (10% glycerol, 50mM HEPES pH7,5; 140mM NaCl; 0,8% NP40;0,25% Triton; 1mM EDTA, Protease Inhibitor Cocktail 1X (PIC) (Complete EDTA-free; Roche) and incubated for 10 min at 4°C under shaking. The cells were subsequently washed in “Wash buffer” (200mM NaCl; 20mM Tris pH8; 0,5mM EGTA; 1mM EDTA, PIC 1X) for 10 min at 4°C under shaking then were resuspended and centrifuged twice during 5 min 1700g at 4°C in “Shearing Buffer” (10mM Tris pH7,6; 1mM EDTA; 0,1%SDS; PIC 1X). Finally, nuclei were resuspended in 1mL of “Shearing Buffer” and were sonicated with a S220 Focused-ultrasonicator (Covaris)

(Power 140W; Duty Off 10%; Burst Cycle 200). Eighty-five µL of the sonication product were kept for the input, 50 µL for analyzes of the sonication efficiency, and 850 µL diluted twice in IP buffer 2X (300mM NaCl, 10mM Tris pH8; 1mM EDTA; 0,1% SDS; 2% Triton) for ChIP. Either two or five ug of Ab were added and incubated overnight at 4°C (see antibodies section). The next day, 50 µL of agarose beads coupled to protein A (Millipore 16–157) or G (Millipore 16–201) were added for 2 h at 4°C under constant shaking. Alternatively, agarose beads were coated with either 2 or 5 ug of antibody before the addition of the sonication product and incubated overnight at 4°C. For V5-tagged proteins, anti-V5 agarose affinity gel (Sigma-Aldrich, A7345) were incubated overnight at 4°C. Beads were then successively washed for 5 min at 4°C under constant shaking once in "low salt" (0.1% SDS, 1% Triton X-100, 2 mM EDTA, 20 mM Tris HCl pH 8.0, 150 mM NaCl) buffer, once in "high salt" (0.1% SDS, 1% Triton X-100, 2 mM EDTA, 20 mM Tris HCl pH 8.0, 500 mM NaCl) buffer, once in "LiCl" (0.25 mM LiCL, 1% NP40, 1% NaDOC, 1 mM EDTA, 10 mM Tris HCl pH 8.0) buffer, and twice in TE (10 mM Tris pH 8.0, 1 mM EDTA) buffer. Chromatin-antibody complexes are then eluted at 65°C for 30 min under constant shaking with 200 µL of elution buffer (1% SDS, 0.1 M NaHCO3). Input and IP products were de-crosslinked overnight at 65°C with 20 mg/mL of RNAse (Sigma) then treated for 2 hours at 55°C with 20 mg/mL of proteinase K (Sigma). DNA was then purified by phenol-chloroform/ethanol precipitation, resuspended in water, and kept at -20°C until use for qPCR.
Quantitative PCRs were performed using the KAPA SYBR qPCR Master Mix (SYBR Green I dye chemistry) (KAPA BIOSYSTEMS, KK4618) and the CFX connect apparatus (Bio-Rad). Primers used are listed below:

HSV-1 genes				
Genes	**Proteins**		**Forward primers (5'-> 3')**	**Reverse primers (5'-> 3')**
UL2	Uracil DNA glycosylase	promoter	TAAACCAACGAAAAGCGCGG	5' GGCACCCACAGAAACCTACA 3'
		CDS	CCCTCTCCAAGGTTCCGTTC	CGACCAGTCGATGGGTGAAA
UL23	TK	promoter	CAGCTGCTTCATCCCCGTGG	AGATCTGCGGCACGCTGTTG
		CDS	ATGCTGCCCATAAGGTATCG	GTAATGACAAGCGCCCAGAT
UL26	VP21	promoter	AGAACAAGAGCCTCCGTTGG	AGGCGAGAGCGAATGCTAAA
		CDS	CCCATTTACGTGGCTGGGTT	TCCGGATCCAATGCCAACTC
UL29	ICP8	promoter	CCTTTTGTCAATCGGTCCGC	CGGGAGACATACCTTGTCGG
UL42	DNA polymerase	promoter	CGTAGTTTCTGGCTCGGTGA	GAACACCCCACAGTGACGAG
		CDS	TGTTCACCACGAGTACCTGC	TTTCCCCGTACACCGTCTTG
LacZ/UL43 (HCMV-lacZ reporter cassette)	β-Galactosidase	Promoter (CMV)	TTCCTACTTGGCAGTACATCTACG	GTCAATGGGGTGGAGACTTGG
		CDS (LacZ)	GCAGCAACGAGACGTCA	GAAAGCTGGCTACAGGAAG
UL44	gC	promoter	CGCCGGTGTGTGATGATTT	TTTATACCCGGGCCCCAT
		CDS	GGGTCCGTCCCCCCCAAT	CGTTAGGTTGGGGGCGCT
UL48	VP16	promoter	GCGTTCATGTCGGCAAACAG	CCCGTATCAACCCCACCCAAT
		CDS	TGCGGGAGCTAAACCACATT	TCCAACTTCGCCCGAATCAA
UL54	ICP27	promoter	CCACGGGTATAAGGACATCCA	GGATATGGCCTCTGGTGGTG

		CDS	GGCGACTGACATTGA	CTGCTGTCCGATTCCAGGTC
LAT	Latency Associated transcript	exon	GGCTCCATCGCCTTTCCT	AAGGGAGGGAGGAGGGTACTG
		intron	CCCACGTACTCCAAGAAGGC	AGACCCAAGCATAGAGAGCCAG
US1	ICP22	promoter	GATCGCATCGGAAAGGGACA	GGTGCTTACCCGTGCAAAAA
		CDS	GTTACGCTGGAAACCCCAGA	CCAGACACTTGCGGTCTTCT
US3	Protein kinase US3	promoter	GCGGGGGCTGCTCTAAAAAT	GGGTTTTAAGGAGCGGCAGT
		CDS	ACTGGCATGGGCTTTACGAT	TTCACGATTACCCGTTGGGG
US6	gD	promoter	GGGGTTAGGGAGTTGTTCGG	CGCACCACACAAAAGAGACC
		CDS	ACGGTTTACTACGCCGTGTT	TGTAGGGTTGTTTCCGGACG
US12	ICP47	promoter	GATCGCATCGGAAAGGGACA	GGTGCTTACCCGTGCAAAAA
		CDS	TACCGGATTACGGGGACTGT	ATAAAAGGGGGCGTGAGGAC

siRNA transfections

Transfections of BJ cells with siRNAs was performed using Lipofectamine RNAiMAX and following the supplier's procedure (Thermo Fisher Scientific). The following siRNAs were used at a final concentration of 40 nM for 48 h: siluc 5'- CGUACGCGGAAUACUUCGA [70], siSETDB1 : 5'ACCCGAGGCUUUGCUCUUA [20].

Reactivation procedures

BJ cells

Cells were transduced with pLKO-tet-On-shRNA to produce BJ-ishRNA cell lines stably and inducibly expressing the ishRNA (selection puro 1 ug/mL). FBS Tetracycline free (Clinisciences, FBS-TET-12A) was used to prevent ishRNA expression. BJ-ishRNA were infected with lqHSV-1 for 4 days at 38.5°C to stabilize the formation of vDCP NBs. Then, the expression of shRNA was induced by the addition of doxycycline (1ug/mL) in the medium. Cells were incubated at 32°C the permissive temperature for *lq*HSV-1 (see section virus). From day 8 to day 10 after addition of doxycycline, the cells were fixed to proceed to immuno-FISH analyses or RNA were extracted to perform RT-qPCR (see section RT-qPCR).

HiPSDN

HiPSDN were cultured for at least 24 hours without antimitotic agents prior to infection with lqHSV-1. HiPSDN were infected with the indicated virus at 3.10e5 PFU/wells for 1h30 at 37°C. Post-infection, inoculum was replaced with neurobasal containing NGF (20ng/ml), NT3 (10ng/ml). After 4 days at 38°C, neurons were transduced with the indicated lentivirus (see lentivirus section). The next day, transduced neurons were put at 32°C (the permissive temperature for replication) during the indicated times. Human Serum (1%) was added to the media to limit cell-to-cell spread. Reactivation was quantified by RT-qPCR of HSV-1 lytic mRNAs isolated from the cells in culture. Same experiment was performed but without Human serum to recover the supernatant. Reactivation was quantified by the production of infectious viral particles through supernatant titration.

RT-qPCR

RNAs were extracted according to The Qiagen RNeasy Mini Kit manufactured protocol (Qiagen, Valencia, CA). RNAs were treated 30mn at 37°C with DNAseI (thermo fisher). Then 1ug was taken to perform RT with RevertAID Reverse Transcriptase (thermo fisher). cDNA was then resuspended in water and kept at -20°C until use for qPCR. Quantitative PCRs were performed using the KAPA SYBR qPCR Master Mix (SYBR Green I dye chemistry) (KAPA BIOSYSTEMS, KK4618) and the CFX connect apparatus (Bio-Rad). Primers used are listed below:

Cellular genes		
Gene	**Forward primers (5'-> 3')**	**Reverse primers (5'-> 3')**
Actin	CGGGAAATCGTGCGTGACATTAAG	GAACCGCTCATTGCCAATGGTGAT
BRN3A	GAAGTGAGTGGGAGCACAGC	CGAAGCTCCGGAATTCTGCT
MORC2	GGATCGAGGAGGATTTAT	GGTCATGGTGTCTTCCTTCTT
MPP8	TCTGGCATCCTGCTGTTTATC	CTGCACTCTGTATGCACCTATT
PPHLN	AAGAAACCACCACTGCTAGAC	CCATCTCTCATGTCCCTGTATTC
SETDB1	CCGCTACCTCAACCACAGTT	CAGCCCGGATTCTTTTGCTG
TASOR	GCATTCCACTTCGGCTTTAAC	CAGAGCACACTCTCTTCTTCTT
TRPV1	GGCTGTCTTCATCATCCTGCTGCT	GTTCTTGCTCTCCTGTGCGATCTTGT
TUJ1	GGCCAAGGGTCACTACACG	GCAGTCGCAGTTTTCACACTC
VGLUT2	AGAAACAACCCTGGGCAGAC	AACCTCCATTGGCCTGTGTT

HSV-1 genes				
Genes	**Proteins**		**Forward primers (5'-> 3')**	**Reverse primers (5'-> 3')**
UL23	TK	CDS	ATGCTGCCCATAAGGTATCG	GTAATGACAAGCGCCCAGAT
LacZ/UL43 (HCMV-lacZ reporter cassette	β-Galactosidase	CDS (LacZ)	GCAGCAACGAGACGTCA	GAAAGCTGGCTACAGGAAG
UL44	gC	CDS	GGGTCCGTCCCCCCCAAT	CGTTAGGTTGGGGGCGCT
UL54	ICP27	CDS	GGCGACTGACATTGA	CTGCTGTCCGATTCCAGGTC
US1	ICP22	CDS	GTTACGCTGGAAACCCCAGA	CCAGACACTTGCGGTCTTCT
US6	gD	CDS	ACGGTTTACTACGCCGTGTT	TGTAGGGTTGTTTCCGGACG

Western blotting

RIPA extracts were obtained by lysing the cells in RIPA buffer (50mM Tris-HCl pH 7.5, 150mM NaCl, 0,5% Na-Deoxycholate, 1% NP-40, 0,1% SDS, 5mM EDTA) supplemented with 1X protease inhibitor cocktail (PIC) for 20min on ice. After incubation, RIPA extracts were centrifugated for 10min at 16000g at 4°C and supernatants were recovered and diluted with 4X LSB (250mM Tris-HCl pH 6.8, 40% glycerol, 8% SDS, bromophenol blue). Protein extracts were boiled for 10 minutes and then loaded on polyacrylamide gels (TGX Stain-Free FastCast gels (Bio-

Rad, 1610181/1610183) or home-made gels) for electrophoresis. Stain-free technology or Ponceau 0,1% (Sigma-Aldrich, P7170) were used to reveal proteins transferred on nitrocellulose membrane with the Trans-Blot Turbo Transfer System (Bio-Rad, 1704150). Membranes were blocked in PBS 0.1% Tween20 (PBST) 5% milk for 30 minutes at RT°C and incubated with primary antibodies diluted in PBST or PBST 5% BSA O/N at 4°C (see antibodies section). After washing the membranes twice in PBST, they were incubated in secondary antibodies conjugated with horseradish peroxidase (HRP) (Dako, P0399, P0447 and P0450) diluted according to supplier recommendations in PBST for 1 hour at RT°C. Signal was revealed on ChemiDoc Imaging System (Bio-Rad) by using Amersham ECL Prime Western Blotting Detection Reagent (GE Healthcare Life Sciences, RPN2236) or Clarity Max Western ECL Blotting Substrate (Bio-Rad, 1705062).

Antibodies

The following primary antibodies were used:

For ChIP :

Proteins	Supplier	Catalog number	Species
Flag	Sigma	f1804	Mouse monoclonal
HA	Abcam	ab9110	Rabbit polyclonal
H3	Abcam	1791	Rabbit polyclonal
H3K9me3	Abcam	ab8898	Rabbit polyclonal
Immunoglobulin G	Diagenode	Kch-504-250	Rabbit polyclonal
MORC2	Bethyl laboratories	A300-149A	Rabbit polyclonal
MPP8	Proteintech	16796-1-AP	Rabbit polyclonal
V5	Sigma	A7345	Mouse monoclonal

For IF :

Proteins	Supplier	Catalog number	Species	Dilution
Flag	Sigma	f1804	Mouse monoclonal (clone M2)	1/200
HA	Abcam	ab9110	Rabbit polyclonal	1/1000
ICP4	Viruzys	P1101	Mouse monoclonal (clone H943)	1/250
MORC2	Sigma	HPA000436	Rabbit polyclonal	1/250
MPP8	Proteintech	16796-1-AP	Rabbit polyclonal	1/400
NeuN	Millipore	MAB377	Mouse monoclonal (clone A60)	1/100
NF200	Sigma	N4142-.2ML	Rabbit polyclonal	1/200

PML	Santa cruz	Sc-966	Mouse monoclonal (PG-M3)	1/250
PML	Sigma	PLA0172	Rabbit polyclonal	1/5000
PPHLN	Sigma	HPA038902	Rabbit polyclonal	1/150
SETDB1	Abcam	ab107225	Mouse monoclonal	1/250
SETDB1	Proteintech	11231-1-AP	Rabbit polyclonal	1/250
TASOR	Sigma	HPA006735	Rabbit polyclonal	1/200
TUJ1	BioLegend	PRB-435P-050	Rabbit polyclonal	1/1000
TRPV1	Alomone labs	ACC030	Rabbit polyclonal	1/200
V5	Thermofisher	R960-25	Mouse monoclonal	1/1000

All secondary antibodies were Alexa Fluor-conjugated and were raised in goats (Invitrogen).

For WB :

Proteins	**Supplier**	**Catalog number**	**Species**
Actin	Sigma	A2066	Rabbit polyclonal
α-actinin	Millipore	05384	Mouse (clone AT6/172)
MORC2	Bethyl laboratories	A300-149A	Rabbit polyclonal
MPP8	Proteintech	16796-1-AP	Rabbit polyclonal
PPHLN	Sigma	HPA038902	Rabbit polyclonal
SETDB1	Proteintech	11231-1-AP	Rabbit polyclonal
TASOR	Sigma	HPA006735	Rabbit polyclonal
α-Tubulin	Sigma	T6199	Mouse monoclonal (clone DM1A)

All secondary antibodies were HRP-conjugated and were raised in goats (Sigma).

Figure legends

Fig. 1 Detection of proteins of the HUSH-SETDB1-MORC2 entity in vDCP NBs. Immuno-FISH to detect proteins of the HUSH-SETDB1-MORC2 (green) entity and PML (blue/grey) together with HSH-1 genomes. BJ cells were infected or not with lqHSV-1 (m.o.i.= 3, 100% of cells infected) and harvested at 4 dpi to perform immuno-FISH. Endogenous SETDB1 and MPP8 were readily detectable with native antibodies supporting the FISH procedure. All other proteins were detected through the expression of an ectopic tagged version. FLAG-MPP8 was also detected as a control for the other HUSH complex components. Insets represent nuclei. Zooms point out vDCP NBs. **a,** detection of endogenous SETDB1. **b,** detection of endogenous MPP8. **c,** detection of FLAG tagged MPP8. **d,** detection of v5 tagged periphilin (PPHLN). **e,** detection of HA tagged TASOR. **f,** detection of v5 tagged MORC2. NI = not infected; Inf. = infected. Scale bar represents 5µm. 100% indicates that all cells show the co-localization of the indicated protein with all the HSV-1 genomes and with PML.

Fig. 2 Interaction of the proteins of the HUSH-SETDB1-MORC2 entity with PML NBs-associated latent HSV-1 genome. a, schematic view of the ChIP procedure to detect interactions of proteins with viral genomes. Control BJ cells or BJ cells expressing a tagged version of proteins of interest were infected with lqHSV-1 (m.o.i.= 3) and ChIP-qPCR was performed 24h pi. All experiments were performed at least 3 times. Measurements were taken from distinct samples. Quantifications data are mean values (+/- SD). P-values * <0.05; ** <0.01 (one-tailed paired Student's t-test). **b, c** interaction of endogenous MPP8 and MORC2 with viral genome loci, respectively. **d,** mean fold enrichments on the different viral loci of the corresponding proteins compared to control BJ cells. For quantification details on each loci see expended supplemental fig. S4.

Fig. 3 Inactivation of proteins of the HUSH-SETDB1-MORC2 entity reduces H3K9me3 mark PML NBs-associated latent HSV-1 genome. a, schematic view of the ChIP procedure to detect enrichment of H3K9me3 on viral genomes after depletion or not by shRNAs of proteins of interest or after expression of HIV-2 Vpx. All experiments were performed at least 3 times. Measurements were taken from distinct samples. Quantifications data are mean values (+/- SD). P-values * <0.05; ** <0.01; *** <0.001 (one-tailed paired Student's t-test). H3K9me3 signal was standardized over total H3 present on each locus. **b-f,** WB on the

target proteins to confirm the efficiency of the specific shRNAs. **g,** mean fold enrichments on the different viral loci of H3K9me3 in specific shRNA-depleted cells compared to cells expressing a control shRNA. For quantification details on each loci see expanded supplemental fig. S5. **h,** WB on TASOR in cells expressing HIV-2 Vpx. **i,** fold enrichment on the different viral loci of H3K9me3 in cells expressing HIV-2 Vpx.

Fig. 4 The HUSH-SETDB1-MORC2 entity maintains the silencing of PML NBs-associated latent HSV-1. a, schematic view of the experimental procedure to determine the restrictive activity of the individual proteins of the HUSH-SETDB1-MORC2 entity. BJ cells expressing inducible shRNA control (shCTRL) or shRNA against a protein of interest were infected with lqHSV-1 (m.o.i.= 3) at 38.5°C to establish latency. Five days later doxycycline was added for 9 days shifting the temperature at 32°C to allow virus replication. Cells were used to perform RT-qPCR to quantify expression of viral lytic genes or immuno-FISH to detect viral RC. **b-f,** RT-qPCR on representative HSV-1 lytic genes following treatment with a shCTRL, or a shRNA inactivating SETDB1, PPHLN, TASOR, MPP8, MORC2, respectively. All experiments were performed at least 3 times. Measurements were taken from distinct samples. Quantifications data are mean values (+/- SD). P-values * <0.05; ** <0.01; *** <0.001 (one-tailed paired Student's t-test). **e**, immuno-FISH allowing the detection of PML (green), HSV-1 (red) and nuclei (grey, DAPI) in cell monolayers after induction of the shRNA CTRL, or targeting HUSH (shMPP8 shown as an example), or MORC2. Scale bar represents 5 µm. RC : replication compartment. **f,** titration on U2OS cells of infectious viral progeny production from above experiments using shRNA CTRL, or a shRNA inactivating each of the protein of the HUSH-SETDB1-MORC2 entity. Up : procedure; down : viral plaques with supernatant from shMORC2 BJ shown as an example. Scale bar represents 100 µm. **g**, numerations of viral plaques from the above conditions.

Fig. 5 Expression of HIV-2 Vpx induces HSV-1 reactivation. a, schematic view of the experimental procedure as described in figure 3.**b,** RT-qPCR on representative HSV-1 lytic genes following treatment with a control (CTRL) or inducible HIV-2 Vpx-expressing plasmid. **c,** BJ cell monolayer showing a viral plaque appearing following HIV-2 Vpx expression. Scale bar represents 100 µm. **d,** immuno-FISH allowing the detection of PML (green), HSV-1 (red) and nuclei (grey, DAPI) following HIV-2 Vpx expression. Scale bar represents 5 µm. RC :

replication compartment**. e,** titration on U2OS cells of infectious viral progeny production as described in figure 3. Up : procedure; down : viral plaques with supernatant from HIV-2 Vpx-expressing BJ. **f,** numeration on U2OS cells of infectious viral progeny production in control BJ vs HIV-2 Vpx-expressing BJ cells. Scale bar represents 100 µm.

Fig. 6 ICP0 induces reactivation when expressed in HSV-1 latently infected neurons. a, schematic view of the experimental procedure in hiPSDN infected with lqHSV-1 at 38.5°C. Four days after infection with lqHSV-1 neurons were transduced with lentiviruses control (CTRL) or expressing ICP0 or ICP0RFmut, and temperature was shifted to 32°C to allow virus replication. Multiple analyses were performed at 3 days post transduction (dpt). **b,** RT-qPCR on representative HSV-1 lytic genes following expression of ICP0 (left) or its non-functional mutant ICP0RFmut (right). All experiments are in triplicates. All quantifications data are mean values (+/- SD). Measurements were taken from distinct samples. P-values * <0.05; ** <0.01; *** <0.001 (one-tailed paired Student's t-test). **c,** Detection of viral plaques on U2OS cell monolayers in contact with supernatants from lqHSV-1 infected neurons transduced for 3dpt with lentivirus CTRL or expressing ICP0 or ICP0RFmut. Crystal violet (grayscale) images for plaques (circled in red) visualization are shown. Scale bar represents 500 µm. **d**, numeration of the plaques detected in **c**. **e,** Immunofluorescent detection of ICP4 (red) and NF200 (green) showing viral RC in neurons. Arrows point out two RCs in the same nucleus of a single neuron. Scale bar represents 10 µm.

Fig. 7 The HUSH-SETDB1-MORC2 entity acts as a restriction pathway in neurons infected with HSV-1. a, schematic view of the experimental procedure to determine the restriction activity of the HUSH-SETDB1-MORC2 entity in hiPSDN infected with lqHSV-1 at 38.5°C. Four days after infection with lqHSV-1 neurons were transduced with lentiviruses expressing a shRNA control, or a shRNA against MORC2, and temperature was shifted to 32°C to allow virus replication. Multiple analyses were performed 5 and 7 days post transduction (dpt). **b,** RT-qPCR at 5dpt (left) and 7dpt (right) on representative HSV-1 lytic genes following treatment with a shRNA CTRL (shCTRL), or a shRNA inactivating MORC2. All experiments are in triplicates. Measurements were taken from distinct samples. All quantifications data are mean values (+/- SD). P-values * <0.05; ** <0.01 (one-tailed paired Student's t-test). **c,** Detection of viral plaques in U2OS cells monolayers in contact with supernatants from

shCTRL (i) or shMORC2 (ii) treated lqHSV-1 infected neurons. Crystal violet (grayscale) images for plaques visualization are shown. Scale bar represents 100 µm. **d,** Numeration of viral plaques from **c**. P-values * <0.05 (one-tailed paired Student's t-test). Measurements were taken from distinct samples. Crystal violet images (grayscale) of U2OS cell layers are shown above each condition. Scale bar represents 500 µm. **e,** model of epigenetic restriction of nuclear incoming HSV-1 DNA by the HUSH-SETDB1-MORC2 entity in association with PML NBs through the apposition of the tri-methyl mark on H3K9 of the chromatinized latent viral genome. Made with Biorender.

Supplementary figure legends

Supplementary Fig.1. SETDB1 is a component of vDCP NBs. a, BJ cells were infected or not (NI) with lqHSV-1 (m.o.i. 3, 100% of cells infected) and harvested at different times post-infection (2, 7 dpi) to perform immunofluorescence to detect SETDB1 (green), PML NBs (red), and nuclei (DAPI, grey). Scale bar represents 5µm. **b,** BJ cells were infected with lqHSV-1 (m.o.i. 3) and harvested at 2 dpi to perform immuno-FISH to detect SETDB1 (green), viral genomes (red), and nuclei (DAPI, grey). Scale bar represents 5µm. 100%, indicates that all infected cells show SETDB1 co-localizing with HSV-1 and PML

Supplementary Fig.2. Ectopically expressed MPP8 co-localizes in vDCP NBs. Immuno-FISH on FLAG-MPP8-expressing BJ cells and infected with lqHSV-1 for 2 days. Immunofluorescence stains FLAG-MPP8 (green) and PML (blue/grey). FISH stained HSV-1 genomes (red). Nucleus is stained by DAPI. Scale bar represents 5µm.

Supplementary Fig.3. Endogenous staining of MPP8, TASOR, PPHLN, MORC2 and PML NBs. a to d, Immunofluorescences on BJ cells of endogenous proteins of interest (green) co-stained with PML (red). Scale bars represent 5µm.

Supplementary Fig.4. Ectopically expressed SETDB1, MPP8, TASOR, PPHLN, MORC2 co-localize with PML NBs. a to e, Immunofluorescences on BJ cells transfected with plasmids

expressing tagged versions of proteins of interest (green) co-stained with PML (red). Scale bars represent 5µm.

Supplementary Fig.5. Endogenous MORC2 interacts with PML NBs-associated latent HSV-1. a, schematic view of the ChIP procedure to detect interactions of proteins with viral genomes. **b,** BJ cells were infected with lqHSV-1 (m.o.i.= 3) and ChIP-qPCR was performed 24h pi. The data show the interaction of endogenous MORC2 with full set of viral genome loci (mean values +/- SD). All experiments were performed at least 3 times. Measurements were taken from distinct samples. P-values * <0.05; ** <0.01 (one-tailed paired Student's t-test).

Supplementary Fig.6. Expanded ChIP data for the interaction of proteins of the HUSH-SETDB1-MORC2 entity with PML NBs-associated latent HSV-1. a, schematic view of the ChIP procedure to detect interactions of proteins with viral genomes. **b to f,** control BJ cells or BJ cells expressing a tagged version of proteins of interest were infected with lqHSV-1 (m.o.i.= 3) and ChIP-qPCR was performed 24h pi. All experiments were performed at least 3 times. Measurements were taken from distinct samples. P-values * <0.05; ** <0.01 (one-tailed paired Student's t-test).

Supplementary Fig.7. Expanded ChIP data for the impact of depletion of the proteins of the HUSH-SETDB1-MORC2 entity on H3K9me3 association with lqHSV-1. a, schematic view of the ChIP procedure to detect interactions of H3K9me3 with viral genomes after depletion or not by shRNAs of proteins of interest. **b to f,** BJ cells expressing a shRNA control or BJ cells expressing a shRNA inactivating a specific protein were infected with lqHSV-1 (m.o.i.= 3) and ChIP-qPCR was performed 24h pi. H3K9me3 signal was standardized over total H3 present on each viral locus. All experiments were performed at least 3 times. Measurements were taken from distinct samples. P-values * <0.05; ** <0.01 (one-tailed paired Student's t-test).

Supplementary Fig. 8. HUSH-SETDB1-MORC2 mRNAs quantification following inducible shRNAs expression. a, schematic view of the experimental procedure to determine the restrictive activity of the individual proteins of the HUSH-SETDB1-MORC2 entity.

b-f, RT-qPCR performed from dox inducible shRNAs expressing cells to quantify SETDB1, PPHLN, TASOR, MPP8, MORC2 mRNA, respectively. All experiments were performed at least 3 times. Measurements were taken from distinct samples. All quantifications data are mean values (+/- SD). P-values * <0.05; ** <0.01; *** <0.001 (one-tailed paired Student's t-test). **e,** representative images of BJ cell monolayers showing viral plaques appearing as a result of virus reactivation and spread, following downregulation of individual proteins by shRNA. Scale bars represents 100 µm. **e**, phase contrast microscopy showing viral plaques in BJ cell monolayers as a result of virus reactivation and spread.

Supplementary Fig. 9. Downregulation of SETDB1 with a siRNA also impact on H3K9me3 association with lqHSV-1. a, RT-qPCR showing the efficiency of the siRNA SETDB1 to reduce SETDB1 mRNA. **b,** WB analysis showing that SETDB1 is impacted at the protein level by the use of the siRNA SETDB1. **c,** schematic view of the ChIP procedure to detect interactions of H3K9me3 with viral genomes after depletion or not by siRNAs of SETDB1 or MORC2. **d,** BJ cells expressing a siRNA control (luciferase) or BJ cells expressing a siRNA inactivating SETDB1 were infected with lqHSV-1 (m.o.i.= 3) and ChIP-qPCR was performed 24h pi. H3K9me3 signal was standardized over total H3 present on each viral locus. Experiments were performed at least 3 times. Measurements were taken from distinct samples. P-values * <0.05; ** <0.01 (one-tailed paired Student's t-test).

Supplementary Fig. 10. hiPSDN have nociceptive neurons characteristics and contain PML NBs. a, Phase contrast images of cultured hiPSC and resulting hiPSDN after differentiation protocol described in the methods section. Scale bar represents 10 µm. **b,** immunofluorescence staining of hiPSDN for three major neuronal markers intermediate neurofilament (NF200), neuronal nuclear antigen (NeuN), and beta-III Tubulin (TUJ1/TUBB3). Scale bar represents 10 µm. **c,** Current-clamp recording of membrane potential in iPSC-derived neurons: example recording of a single action potential evoked by current injection of 200 pA for 50 ms. Application of TTX blocked the generation of action potentials. **d,** Representative RT-qPCR (N=3) to measure the relative fold increase in the expression of neuronal (TUJ1/TUBB3) and sensory (BRN3A, vGLUT2, TRKA) neurons from d0 (hiPSC) to d15 (hiPSDN). **e,** RT-qPCR (N=3) to measure the relative fold increase over time in the expression of the TRPV1 receptor, a marker of nociceptive neurons. **f,** immunofluorescence staining of

the TRPV1 receptor in hiPSDN. Scale bar represents 10 µm. **g,** functional analysis of nociceptive hiPSDN for their capacity to respond to capsaicin stimulus by the secretion of CGRP peptide. **h,** immunofluorescence staining showing the presence of native PML NBs (red) in hiPSDN (NF200, green). Scale bar represents 10 µm.

Supplementary Fig. 11. MORC2 shRNA efficiently reduces MORC2 mRNA in iPSDN.
a, schematic view of the experimental procedure as described in figure 6. **b**, RT-qPCR at 5dpt (left) and 7dpt (right) for the quantification of MORC2 mRNAs. Experiments are in triplicates. Measurements were taken from distinct samples. Quantifications data are mean values (+/- SD). P-values *** <0.001 (one-tailed paired Student's t-test).

References

1. Knipe, D. M. & Cliffe, A. Chromatin control of herpes simplex virus lytic and latent infection. *Nat Rev Microbiol* 6, 211–221 (2008).

2. LOMONTE, P. Herpesvirus Latency: On the Importance of Positioning Oneself. *Advances in anatomy, embryology, and cell biology* 223, 95–117 (2017).

3. Catez, F. *et al.* HSV-1 Genome Subnuclear Positioning and Associations with Host-Cell PML-NBs and Centromeres Regulate LAT Locus Transcription during Latency in Neurons. *PLoS Pathog* 8, e1002852 (2012).

4. Maroui, M.-A. *et al.* Latency Entry of Herpes Simplex Virus 1 Is Determined by the Interaction of Its Genome with the Nuclear Environment. *PLoS Pathog* 12, e1005834 (2016).

5. Corpet, A. *et al.* PML nuclear bodies and chromatin dynamics: catch me if you can! *Nucleic Acids Res* 389, 251 (2020).

6. Everett, R. D., Murray, J., Orr, A. & Preston, C. M. Herpes simplex virus type 1 genomes are associated with ND10 nuclear substructures in quiescently infected human fibroblasts. *Journal of virology* 81, 10991–11004 (2007).

7. Alandijany, T. *et al.* Distinct temporal roles for the promyelocytic leukaemia (PML) protein in the sequential regulation of intracellular host immunity to HSV-1 infection. *PLoS Pathog* 14, e1006769 (2018).

8. Cohen, C. *et al.* Promyelocytic leukemia (PML) nuclear bodies (NBs) induce latent/quiescent HSV-1 genomes chromatinization through a PML NB/Histone H3.3/H3.3 Chaperone Axis. *PLoS Pathog* 14, e1007313 (2018).

9. Everett, R. D. *et al.* A novel ubiquitin-specific protease is dynamically associated with the PML nuclear domain and binds to a herpesvirus regulatory protein. *Embo J* 16, 1519–30. (1997).

10. Halford, W. P. & Schaffer, P. A. ICP0 is required for efficient reactivation of herpes simplex virus type 1 from neuronal latency. *Journal of virology* 75, 3240–9. (2001).

11. Thompson, R. L. & Sawtell, N. M. Evidence that the herpes simplex virus type 1 ICP0 protein does not initiate reactivation from latency in vivo. *Journal of virology* 80, 10919–10930 (2006).

12. Boutell, C. *et al.* A Viral Ubiquitin Ligase Has Substrate Preferential SUMO Targeted Ubiquitin Ligase Activity that Counteracts Intrinsic Antiviral Defence. *PLoS Pathog* 7, e1002245 (2011).

13. Wang, Q.-Y. *et al.* Herpesviral latency-associated transcript gene promotes assembly of heterochromatin on viral lytic-gene promoters in latent infection. *Proceedings of the National Academy of Sciences of the United States of America* 102, 16055–16059 (2005).

14. Rea, S. *et al.* Regulation of chromatin structure by site-specific histone H3 methyltransferases. *Nature* 406, 593–599 (2000).

15. Yang, L. *et al.* Molecular cloning of ESET, a novel histone H3-specific methyltransferase that interacts with ERG transcription factor. *Oncogene* 21, 148–152 (2002).

16. Binda, O. On your histone mark, SET, methylate! *Epigenetics : official journal of the DNA Methylation Society* 8, 457–463 (2013).

17. Cho, S., Park, J. S. & Kang, Y.-K. Dual functions of histone-lysine N-methyltransferase Setdb1 protein at promyelocytic leukemia-nuclear body (PML-NB): maintaining PML-NB structure and regulating the expression of its associated genes. *J Biol Chem* 286, 41115–41124 (2011).

18. Matsui, T. *et al.* Proviral silencing in embryonic stem cells requires the histone methyltransferase ESET. *Nature* 464, 927–931 (2010).

19. Rauwel, B. *et al.* Release of human cytomegalovirus from latency by a KAP1/TRIM28 phosphorylation switch. *eLife* 4, 1208 (2015).

20. Tchasovnikarova, I. A. *et al.* GENE SILENCING. Epigenetic silencing by the HUSH complex mediates position-effect variegation in human cells. *Science* 348, 1481–1485 (2015).

21. Seczynska, M., Bloor, S., Cuesta, S. M. & Lehner, P. J. Genome surveillance by HUSH-mediated silencing of intronless mobile elements. *Nature* 1–9 (2021) doi:10.1038/s41586-021-04228-1.

22. Robbez-Masson, L. *et al.* The HUSH complex cooperates with TRIM28 to repress young retrotransposons and new genes. *Genome Res* 28, 836–845 (2018).

23. Liu, N. *et al.* Selective silencing of euchromatic L1s revealed by genome-wide screens for L1 regulators. *Nature* 553, 228–232 (2018).

24. Chougui, G. *et al.* HIV-2/SIV viral protein X counteracts HUSH repressor complex. *Nature microbiology* 3, 891–897 (2018).

25. Zhu, Y., Wang, G. Z., Cingöz, O. & Goff, S. P. NP220 mediates silencing of unintegrated retroviral DNA. *Nature* 564, 278–282 (2018).

26. Cruz-Tapias, P., Robin, P., Pontis, J., Maestro, L. D. & Ait-Si-Ali, S. The H3K9 Methylation Writer SETDB1 and its Reader MPP8 Cooperate to Silence Satellite DNA Repeats in Mouse Embryonic Stem Cells. *Genes* 10, 750 (2019).

27. Das, A. *et al.* Epigenetic Silencing of Recombinant Adeno-associated Virus Genomes by NP220 and the HUSH Complex. *J Virol* 96, e0203921 (2022).

28. Tchasovnikarova, I. A. *et al.* Hyperactivation of HUSH complex function by Charcot-Marie-Tooth disease mutation in MORC2. *Nat Genet* 49, 1035–1044 (2017).

29. Douse, C. H. *et al.* Neuropathic MORC2 mutations perturb GHKL ATPase dimerization dynamics and epigenetic silencing by multiple structural mechanisms. *Nat Commun* 9, 651 (2018).

30. Shao, Y. *et al.* Involvement of histone deacetylation in MORC2-mediated down-regulation of carbonic anhydrase IX. *Nucleic Acids Res* 38, 2813–2824 (2010).

31. Li, D.-Q. *et al.* MORC2 Signaling Integrates Phosphorylation-Dependent, ATPase-Coupled Chromatin Remodeling during the DNA Damage Response. *Cell Reports* 2, 1657–1669 (2012).

32. Albulym, O. M. *et al.* MORC2 mutations cause axonal Charcot–Marie–Tooth disease with pyramidal signs. *Ann Neurol* 79, 419–427 (2016).

33. Ray-Gallet, D. *et al.* Dynamics of histone h3 deposition in vivo reveal a nucleosome gap-filling mechanism for h3.3 to maintain chromatin integrity. *Mol Cell* 44, 928–941 (2011).

34. Banumathy, G. *et al.* Human UBN1 Is an Ortholog of Yeast Hpc2p and Has an Essential Role in the HIRA/ASF1a Chromatin-Remodeling Pathway in Senescent Cells. *Mol Cell Biol* 29, (2009).

35. Ye, X. *et al.* Downregulation of Wnt signaling is a trigger for formation of facultative heterochromatin and onset of cell senescence in primary human cells. *Mol Cell* 27, 183–196 (2007).

36. Banani, S. F. *et al.* Compositional Control of Phase-Separated Cellular Bodies. *Cell* 166, 651–663 (2016).

37. Kleijwegt, C. *et al.* Interplay between PML NBs and HIRA for H3.3 deposition on transcriptionally active interferon-stimulated genes. *Biorxiv* 2021.11.30.470516 (2021) doi:10.1101/2021.11.30.470516.

38. Yurkovetskiy, L. *et al.* Primate immunodeficiency virus proteins Vpx and Vpr counteract transcriptional repression of proviruses by the HUSH complex. *Nat Microbiol* 3, 1354–1361 (2018).

39. Readhead, B. *et al.* Multiscale Analysis of Independent Alzheimer's Cohorts Finds Disruption of Molecular, Genetic, and Clinical Networks by Human Herpesvirus. *Neuron* 99, 64-82.e7 (2018).

40. Itzhaki, R. F., Golde, T. E., Heneka, M. T. & Readhead, B. Do infections have a role in the pathogenesis of Alzheimer disease? *Nat Rev Neurol* 16, 193–197 (2020).

41. Elsässer, S. J., Noh, K.-M., Diaz, N., Allis, C. D. & Banaszynski, L. A. Histone H3.3 is required for endogenous retroviral element silencing in embryonic stem cells. *Nature* 522, 240–244 (2015).

42. Navarro, C., Lyu, J., Katsori, A.-M., Caridha, R. & Elsässer, S. J. An embryonic stem cell-specific heterochromatin state promotes core histone exchange in the absence of DNA accessibility. *Nature communications* 11, 5095 (2020).

43. Jacquier, A., Roubille, S., Lomonte, P. & Schaeffer, L. Microrchidia CW-Type Zinc Finger 2, a Chromatin Modifier in a Spectrum of Peripheral Neuropathies. *Front Cell Neurosci* 16, 896854 (2022).

44. Tan, S.-L. *et al.* Essential roles of the histone methyltransferase ESET in the epigenetic control of neural progenitor cells during development. *Development* 139, 3806–3816 (2012).

45. Hagelkruys, A. *et al.* The HUSH complex controls brain architecture and protocadherin fidelity. *Sci Adv* 8, eabo7247 (2022).

46. Everett, R. D. & Maul, G. G. HSV-1 IE protein Vmw110 causes redistribution of PML. *Embo J* 13, 5062–5069 (1994).

47. Lee, J. S., Raja, P. & Knipe, D. M. Herpesviral ICP0 Protein Promotes Two Waves of Heterochromatin Removal on an Early Viral Promoter during Lytic Infection. *MBio* 7, e02007-15 (2016).

48. Raja, P. *et al.* A Herpesviral Lytic Protein Regulates the Structure of Latent Viral Chromatin. *MBio* 7, e00633-16 (2016).

49. Kwiatkowski, D. L., Thompson, H. W. & Bloom, D. C. The polycomb group protein Bmi1 binds to the herpes simplex virus 1 latent genome and maintains repressive histone marks during latency. *Journal of virology* 83, 8173–8181 (2009).

50. Cliffe, A. R., Coen, D. M. & Knipe, D. M. Kinetics of facultative heterochromatin and polycomb group protein association with the herpes simplex viral genome during establishment of latent infection. 4, (2013).

51. Thompson, R. L., Preston, C. M. & Sawtell, N. M. De novo synthesis of VP16 coordinates the exit from HSV latency in vivo. *PLoS Pathog* 5, e1000352 (2009).

52. Diemen, F. R. van *et al.* CRISPR/Cas9-Mediated Genome Editing of Herpesviruses Limits Productive and Latent Infections. *Plos Pathog* 12, e1005701 (2016).

53. Roehm, P. C. *et al.* Inhibition of HSV-1 Replication by Gene Editing Strategy. *Sci Rep-uk* 6, 23146 (2016).

54. Aubert, M. *et al.* Gene editing and elimination of latent herpes simplex virus in vivo. *Nature communications* 11, 4148 (2020).

55. Chapellier, B. *et al.* Meganuclease targeting HSV-1 protects against herpetic keratitis: Application to corneal transplants. *Mol Ther - Nucleic Acids* 30, 511–521 (2022).

56. Chougui, G. & Margottin-Goguet, F. HUSH, a Link Between Intrinsic Immunity and HIV Latency. *Frontiers in microbiology* 10, 224 (2019).

57. Preston, C. M. Abnormal properties of an immediate early polypeptide in cells infected with the herpes simplex virus type 1 mutant tsK. *Journal of virology* 32, 357–369 (1979).

58. Ace, C., McKee, T., Ryan, J., Cameron, J. & Preston, C. Construction and Characterization of a Herpes Simplex Virus Type 1 Mutant Unable To Transinduce Immediate-Early Gene Expression. *Journal of virology* 63, 2260–2269 (1989).

59. Preston, C. M., Rinaldi, A. & Nicholl, M. J. Herpes simplex virus type 1 immediate early gene expression is stimulated by inhibition of protein synthesis. *J Gen Virol* 79 (Pt 1), 117–124 (1998).

60. Preston, C. M. & Nicholl, M. J. Human Cytomegalovirus Tegument Protein pp71 Directs Long-Term Gene Expression from Quiescent Herpes Simplex Virus Genomes. *Journal of virology* 79, 525–535 (2005).

61. McFarlane, M., Daksis, J. I. & Preston, C. M. Hexamethylene bisacetamide stimulates herpes simplex virus immediate early gene expression in the absence of trans-induction by Vmw65. *J Gen Virol* 73 (Pt 2), 285–292 (1992).

62. Badja, C. *et al.* Efficient and cost-effective generation of mature neurons from human induced pluripotent stem cells. *Stem cells translational medicine* 3, 1467–1472 (2014).

63. Cai, S., Han, L., Ao, Q., Chan, Y.-S. & Shum, D. K.-Y. Human Induced Pluripotent Cell-Derived Sensory Neurons for Fate Commitment of Bone Marrow-Derived Schwann Cells: Implications for Remyelination Therapy. *Stem cells translational medicine* 6, 369–381 (2017).

64. Pear, W. Transient transfection methods for preparation of high-titer retroviral supernatants. *Current protocols in molecular biology* Chapter 9, Unit9.11 (2001).

65. Greenwood, E. J. D. *et al.* Promiscuous Targeting of Cellular Proteins by Vpr Drives Systems-Level Proteomic Remodeling in HIV-1 Infection. *Cell reports* 27, 1579-1596.e7 (2019).

66. Everett, R., Parsy, M. & Orr, A. Analysis of the functions of herpes simplex virus type 1 regulatory protein ICP0 that are critical for lytic infection and derepression of quiescent viral genomes. 83, (2009).

67. Binda, O. *et al.* Trimethylation of histone H3 lysine 4 impairs methylation of histone H3 lysine 9: regulation of lysine methyltransferases by physical interaction with their substrates. *Epigenetics : official journal of the DNA Methylation Society* 5, 767–775 (2010).

68. Cunningham, C. & Davison, A. J. A cosmid-based system for constructing mutants of herpes simplex virus type 1. *Virology* 197, 116–124 (1993).

69. Catez, F., Rousseau, A., Labetoulle, M. & LOMONTE, P. Detection of the genome and transcripts of a persistent DNA virus in neuronal tissues by fluorescent in situ hybridization combined with immunostaining. *Journal of visualized experiments : JoVE* e51091 (2014) doi:10.3791/51091.

70. Adam, S., Polo, S. E. & Almouzni, G. How to restore chromatin structure and function in response to DNA damage? Let the chaperones play. *The FEBS journal* (2014) doi:10.1111/febs.12793.

Acknowledgements

We thank Prof. Roger Everett (Center for Virus Research, University of Glasgow, UK) for the *in*1374/lqHSV-1 virus and ICP0-expressing lentivirus vectors, Dr. Slimane Ait-Si-Ali (Epigenetic and cell fate, University Paris Diderot, France) for SETDB1 constructs.

INMG-PGNM laboratory is funded by grants from the Centre National de la Recherche Scientifique (CNRS), Institut National de la Santé et de la Recherche Médicale (Inserm), University Claude Bernard Lyon 1, and AFM-téléthon. This work was supported by the French National Agency for Research-ANR through grants ANR-18-CE15-0014-01, ANR-20-COV9-0004-01, ANR-21-CE17-0018, LabEX DEV2CAN (ANR-10-LABX-61), ligue contre le cancer, and ANRS (ECTZ188412, ECTZ159208), AFM-téléthon (MyoNeuRALP2). PJL is supported by a Wellcome Trust Principal Research Fellowship ((210688/Z/18/Z). PL is a CNRS Research Director.

Author contributions

S.R., F.J., P.J.L., P.L. conceived the study. S.R., F.J., M. L., F.M., P.J.L., P.L. designed experiments and interpreted data. S.R., F.J., T.E., O.B., C.C., P.T., N.O., O.H., O.P., Y.G., M.L. performed experiments. F.M. developed the hiPSC and contributed to the hiPSDN differentiation protocol. A.C, S.B. contributed to the development and production of lentiviruses. A.C. contributed to the design and performance of experiments in human primary cells. O.P. performed the electrophysiological experiments for hiPSDN. S.R., P.J.L. and P.L. wrote the paper. All authors reviewed and edited the manuscript.

Competing interests

The authors declare no competing interests.

Data availability statement

The datasets generated and/or analysed during the current study are available from the corresponding author on reasonable request.

Figure 1

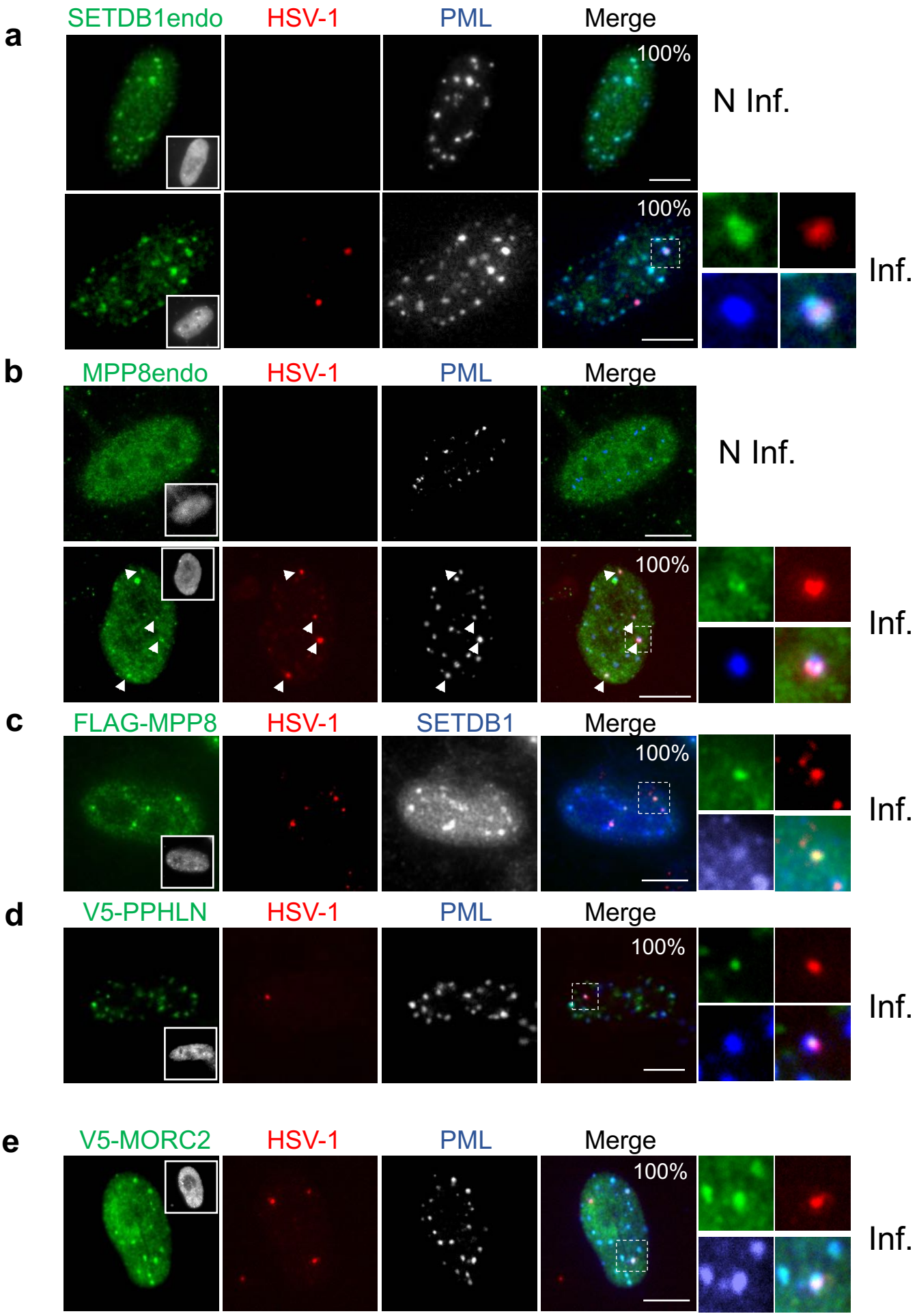
a
SETDB1endo
HSV-1
PML
Merge
100%
N Inf.
100%
Inf.
b
MPP8endo
HSV-1
PML
Merge
N Inf.
100%
Inf.
c
FLAG-MPP8
HSV-1
SETDB1
Merge
100%
Inf.
d
V5-PPHLN
HSV-1
PML
Merge
100%
Inf.
e
V5-MORC2
HSV-1
PML
Merge
100%
Inf.

Figure 2

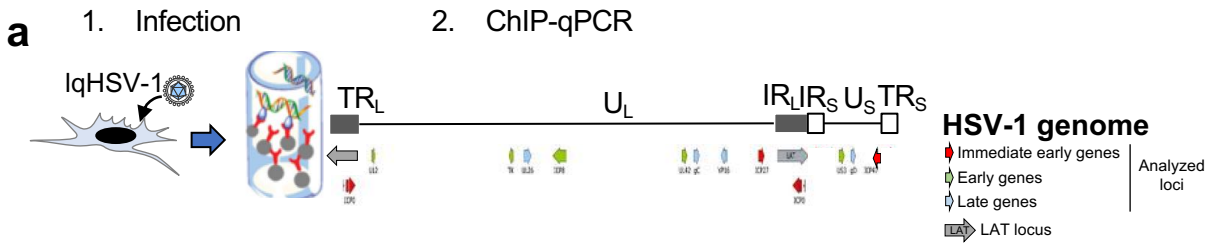
a
1. Infection
2. ChIP-qPCR
lqHSV-1
TRL
UL
IRLIRS US TRS
HSV-1 genome
Immediate early genes
Early genes
Late genes
LAT locus
Analyzed loci

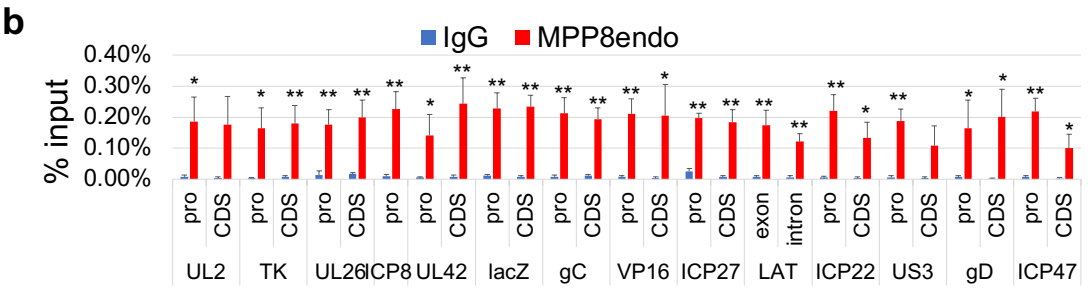
b
IgG
MPP8endo
% input
0.40%
0.30%
0.20%
0.10%
0.00%
pro
CDS
exon
intron
UL2
TK
UL26
ICP8
UL42
lacZ
gC
VP16
ICP27
LAT
ICP22
US3
gD
ICP47

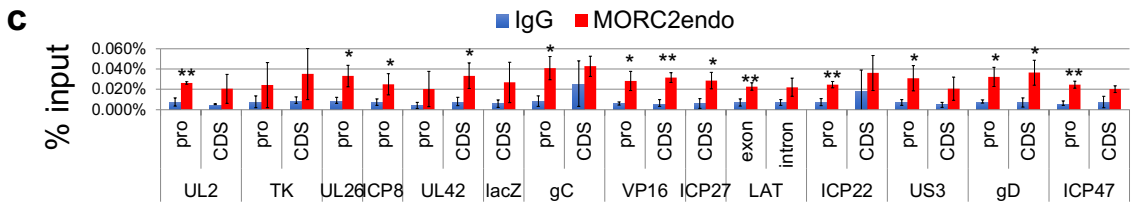
c
IgG
MORC2endo
% input
0.060%
0.040%
0.020%
0.000%
pro
CDS
exon
intron
UL2
TK
UL26
ICP8
UL42
lacZ
gC
VP16
ICP27
LAT
ICP22
US3
gD
ICP47

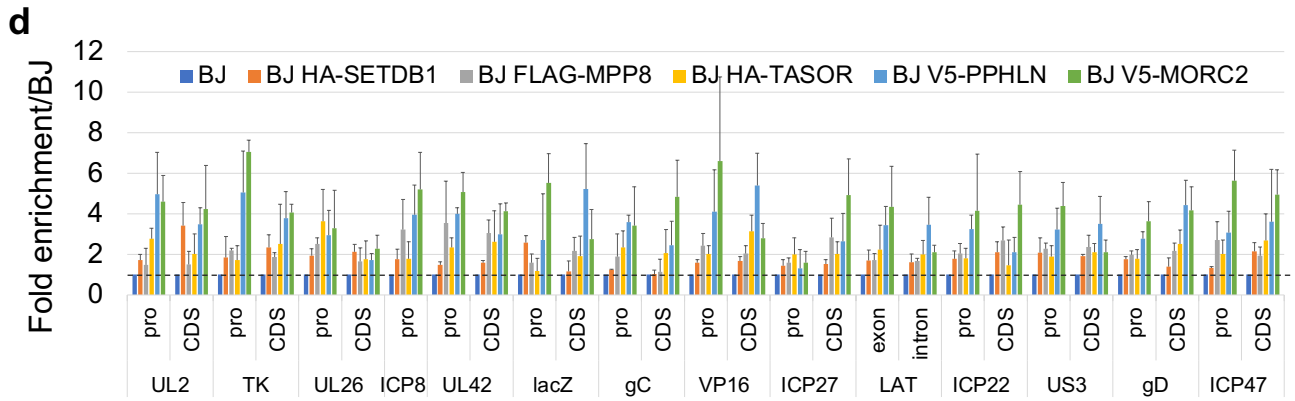
d
BJ
BJ HA-SETDB1
BJ FLAG-MPP8
BJ HA-TASOR
BJ V5-PPHLN
BJ V5-MORC2
Fold enrichment/BJ
12
10
8
6
4
2
0
pro
CDS
exon
intron
UL2
TK
UL26
ICP8
UL42
lacZ
gC
VP16
ICP27
LAT
ICP22
US3
gD
ICP47

Figure 3

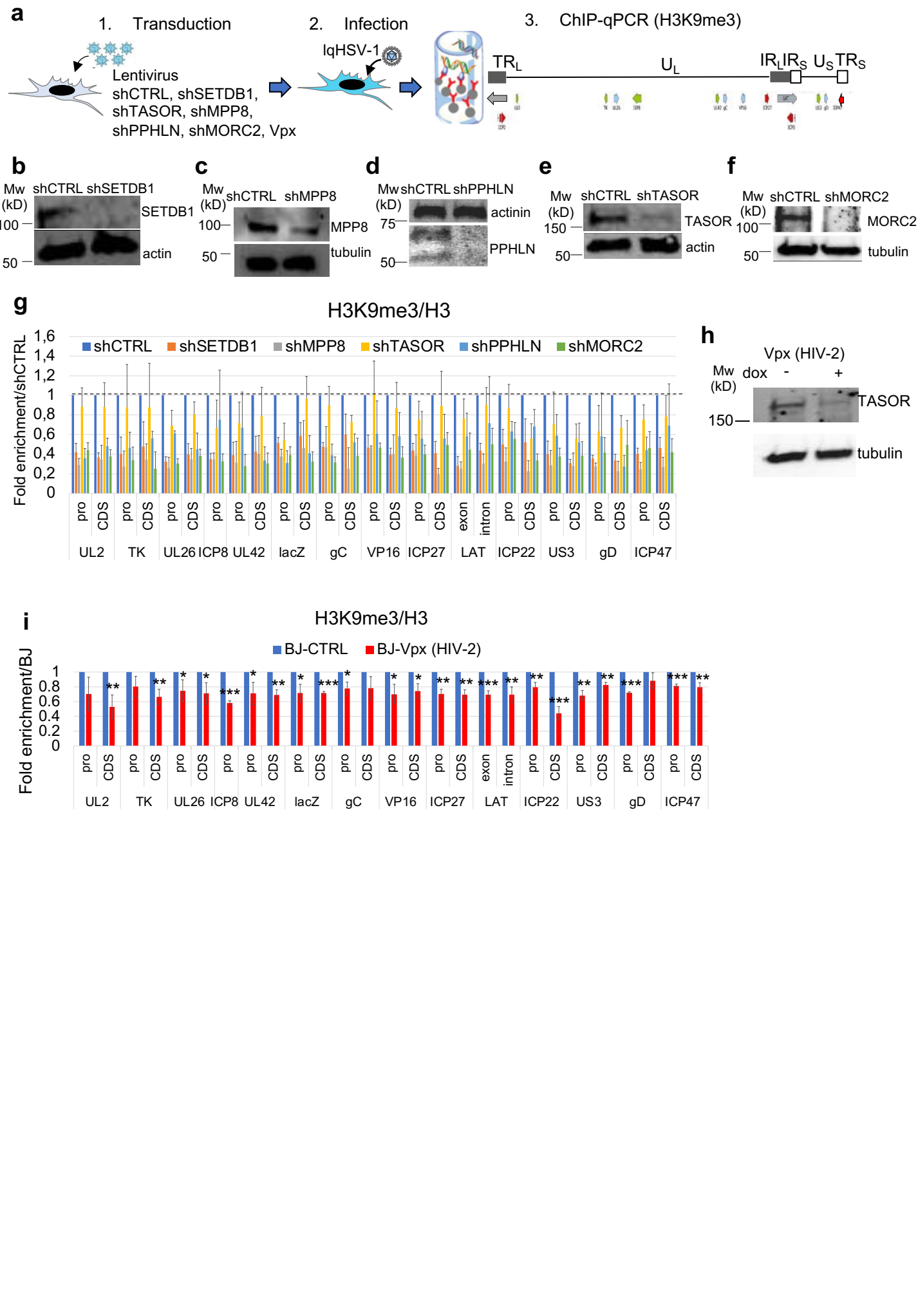
a
1. Transduction
Lentivirus
shCTRL, shSETDB1,
shTASOR, shMPP8,
shPPHLN, shMORC2, Vpx
2. Infection
lqHSV-1
3. ChIP-qPCR (H3K9me3)
TRL
UL
IRLIRS
US
TRS
b
Mw (kD)
shCTRL
shSETDB1
SETDB1
actin
100
50
c
Mw (kD)
shCTRL
shMPP8
MPP8
tubulin
100
50
d
Mw (kD)
shCTRL
shPPHLN
actinin
PPHLN
75
50
e
Mw (kD)
shCTRL
shTASOR
TASOR
actin
150
50
f
Mw (kD)
shCTRL
shMORC2
MORC2
tubulin
100
50
g
H3K9me3/H3
shCTRL
shSETDB1
shMPP8
shTASOR
shPPHLN
shMORC2
Fold enrichment/shCTRL
1,6
1,4
1,2
1
0,8
0,6
0,4
0,2
0
pro
CDS
exon
intron
UL2
TK
UL26
ICP8
UL42
lacZ
gC
VP16
ICP27
LAT
ICP22
US3
gD
ICP47
h
Vpx (HIV-2)
Mw (kD)
dox
-
+
150
TASOR
tubulin
i
H3K9me3/H3
BJ-CTRL
BJ-Vpx (HIV-2)
Fold enrichment/BJ
1
0.8
0.6
0.4
0.2
0
UL2
TK
UL26
ICP8
UL42
lacZ
gC
VP16
ICP27
LAT
ICP22
US3
gD
ICP47

Figure 4

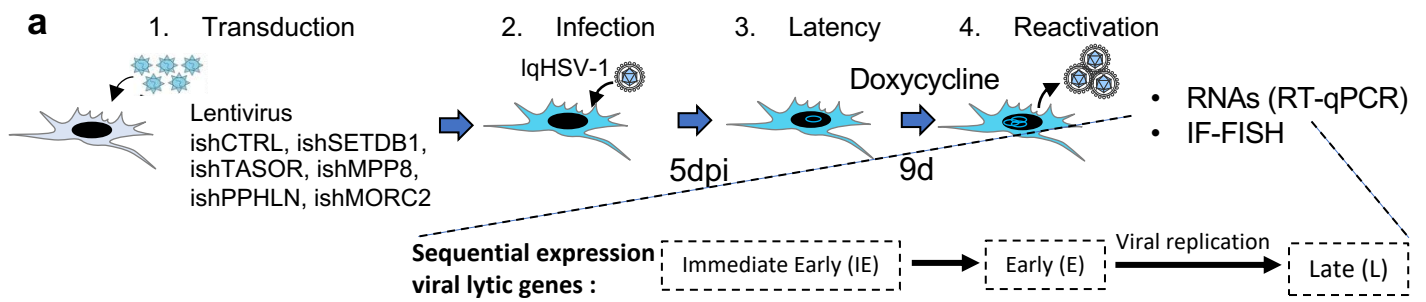
a
1. Transduction
2. Infection
3. Latency
4. Reactivation
Lentivirus
ishCTRL, ishSETDB1,
ishTASOR, ishMPP8,
ishPPHLN, ishMORC2
lqHSV-1
5dpi
Doxycycline
9d
• RNAs (RT-qPCR)
• IF-FISH
Sequential expression
viral lytic genes :
Immediate Early (IE)
Early (E)
Viral replication
Late (L)

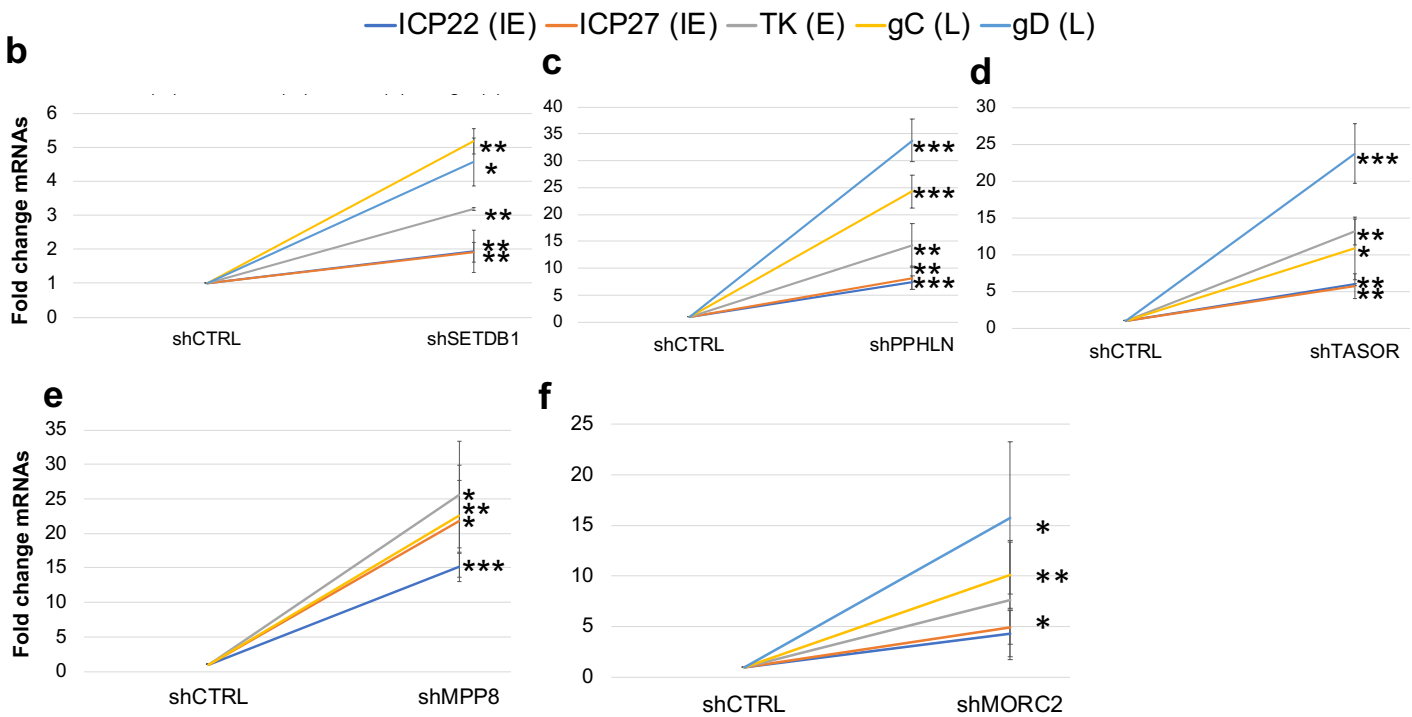
ICP22 (IE)
ICP27 (IE)
TK (E)
gC (L)
gD (L)
b
c
d
e
f
Fold change mRNAs
shCTRL
shSETDB1
shPPHLN
shTASOR
shMPP8
shMORC2

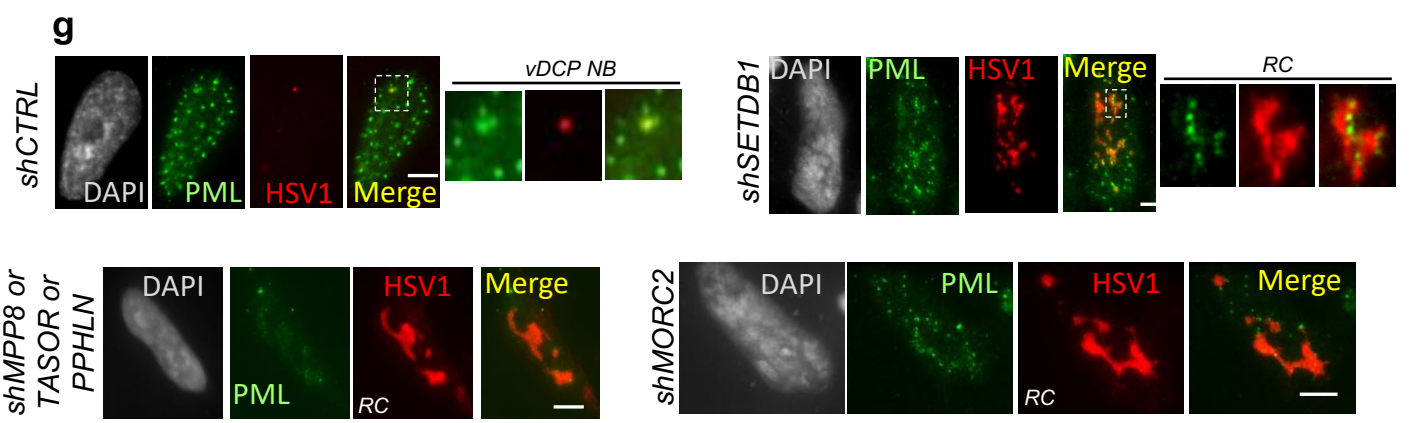
g
shCTRL
shSETDB1
shMPP8 or TASOR or PPHLN
shMORC2
DAPI
PML
HSV1
Merge
vDCP NB
RC

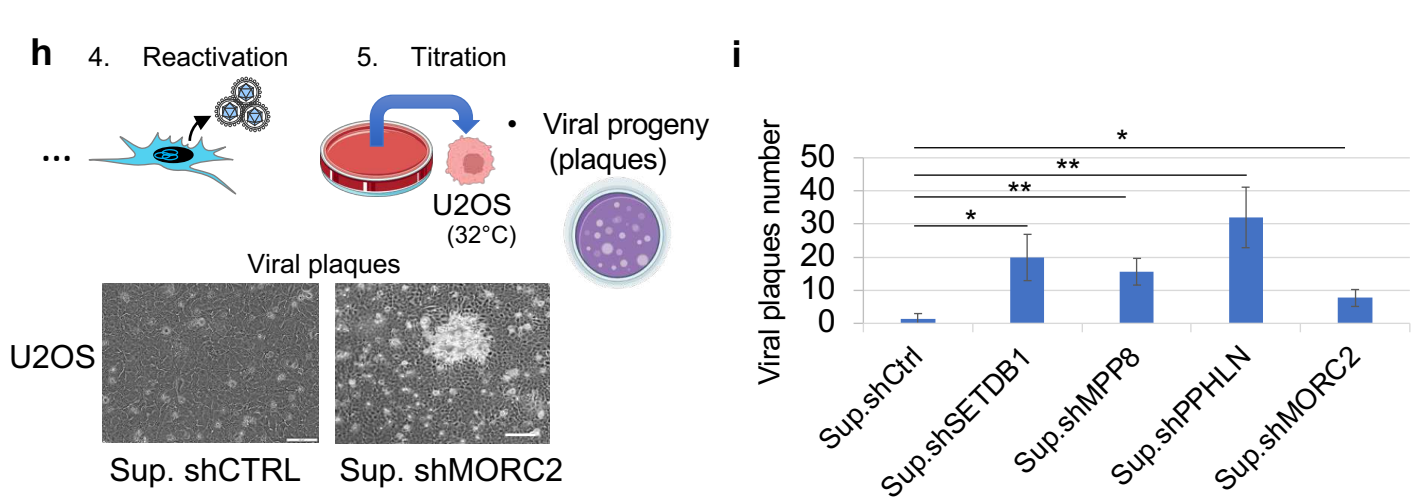
h
4. Reactivation
5. Titration
• Viral progeny (plaques)
U2OS
(32°C)
Viral plaques
U2OS
Sup. shCTRL
Sup. shMORC2
i
Viral plaques number
Sup.shCtrl
Sup.shSETDB1
Sup.shMPP8
Sup.shPPHLN
Sup.shMORC2

Figure 5

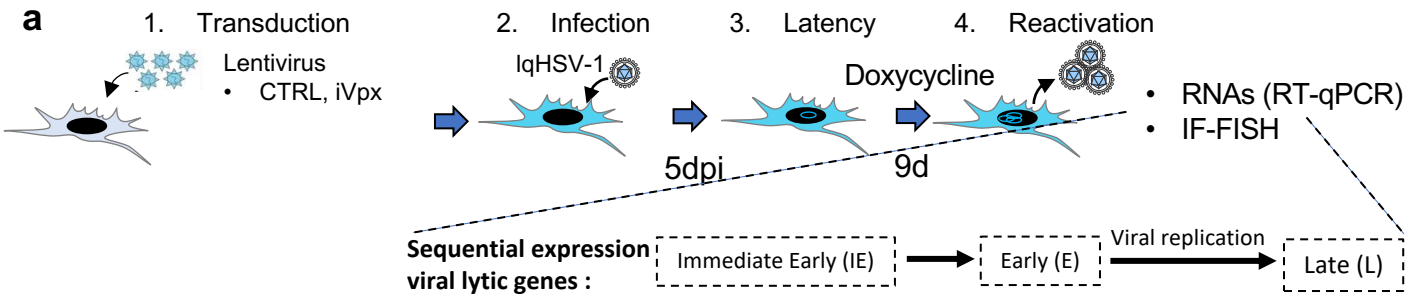
a
1. Transduction
Lentivirus
• CTRL, iVpx
2. Infection
IqHSV-1
5dpi
3. Latency
Doxycycline
9d
4. Reactivation
• RNAs (RT-qPCR)
• IF-FISH
Sequential expression viral lytic genes :
Immediate Early (IE)
Early (E)
Viral replication
Late (L)

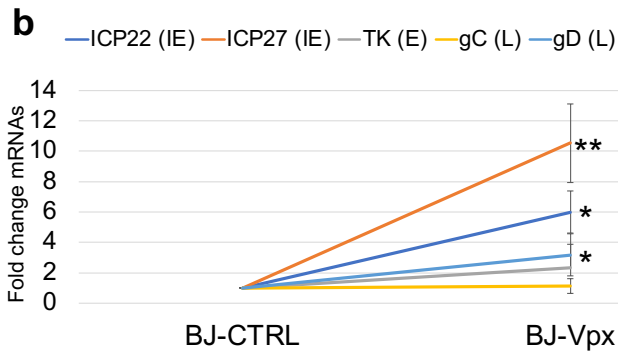
b
ICP22 (IE)
ICP27 (IE)
TK (E)
gC (L)
gD (L)
Fold change mRNAs
14
12
10
8
6
4
2
0
**
*
*
BJ-CTRL
BJ-Vpx

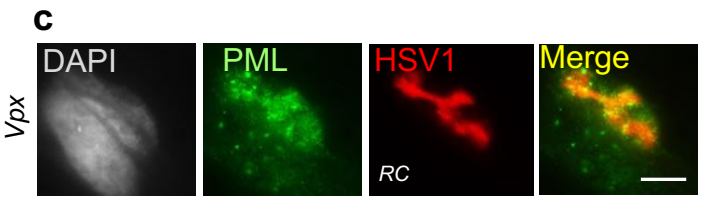
c
Vpx
DAPI
PML
HSV1
Merge
RC

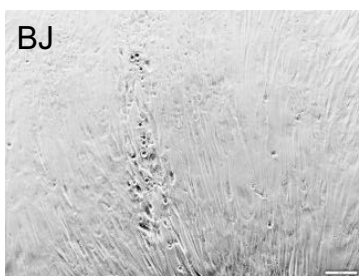
d
BJ

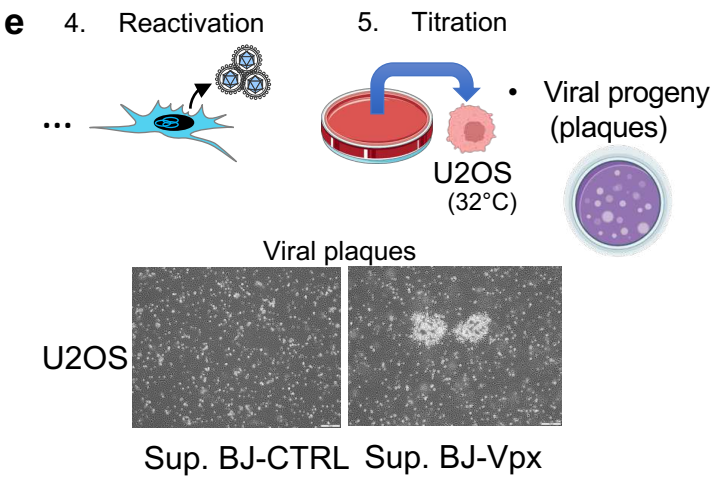
e
4. Reactivation
5. Titration
• Viral progeny (plaques)
U2OS
(32°C)
Viral plaques
U2OS
Sup. BJ-CTRL
Sup. BJ-Vpx

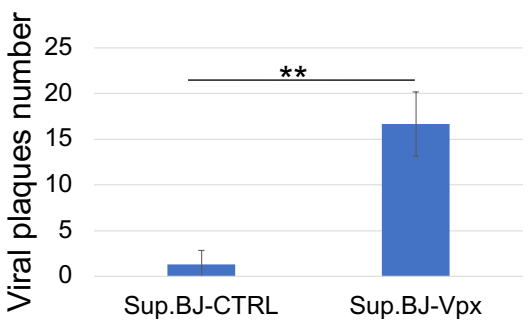
f
Viral plaques number
25
20
15
10
5
0
**
Sup.BJ-CTRL
Sup.BJ-Vpx

Figure 6

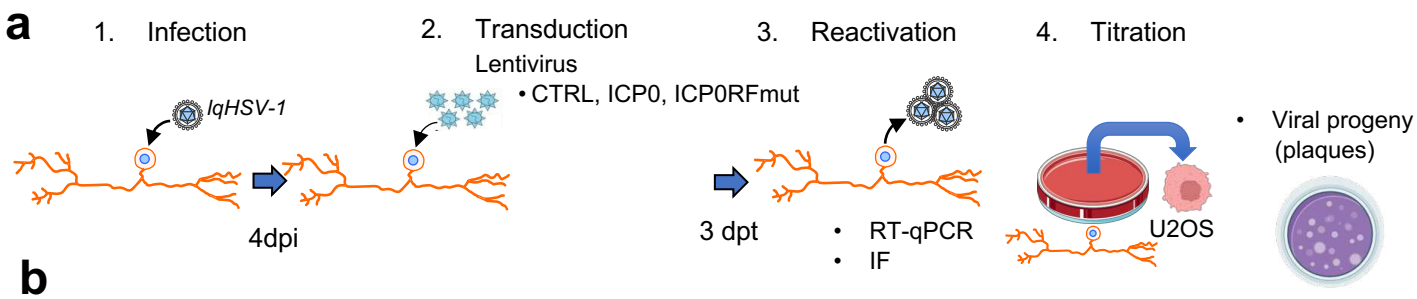
a
1. Infection
2. Transduction
Lentivirus
• CTRL, ICP0, ICP0RFmut
3. Reactivation
4. Titration
lqHSV-1
4dpi
3 dpt
• RT-qPCR
• IF
U2OS
• Viral progeny (plaques)

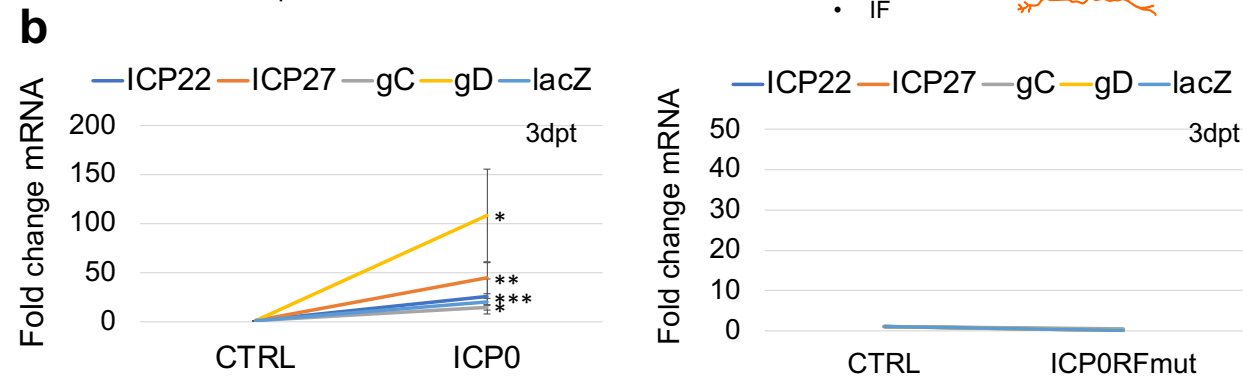
b
ICP22 ICP27 gC gD lacZ
Fold change mRNA
3dpt
CTRL
ICP0
ICP0RFmut

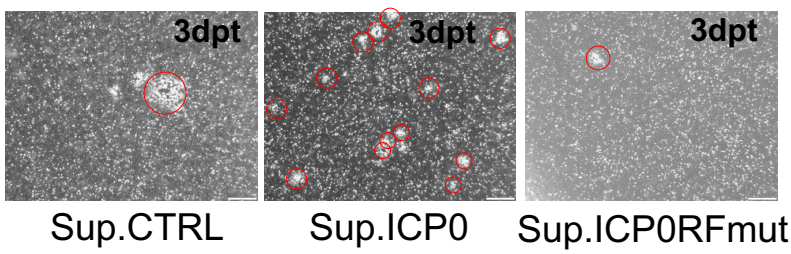
c
3dpt
Sup.CTRL
Sup.ICP0
Sup.ICP0RFmut

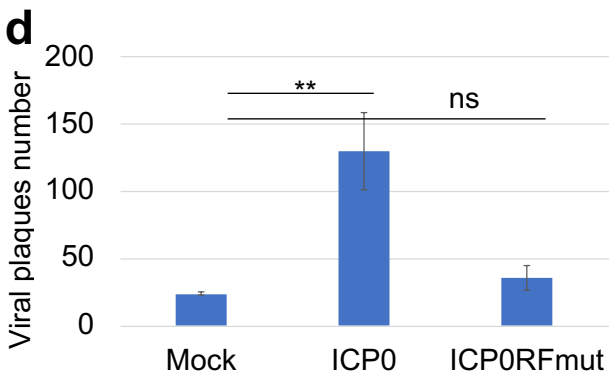
d
Viral plaques number
**
ns
Mock
ICP0
ICP0RFmut

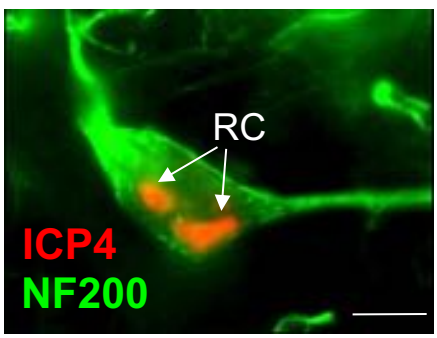
e
RC
ICP4
NF200

Figure 7

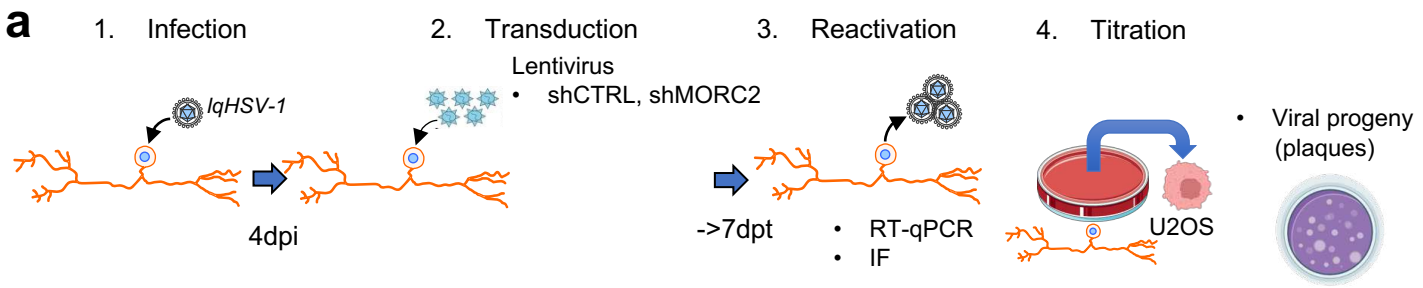
a
1. Infection
2. Transduction
3. Reactivation
4. Titration
lqHSV-1
Lentivirus
• shCTRL, shMORC2
4dpi
->7dpt
• RT-qPCR
• IF
U2OS
• Viral progeny (plaques)

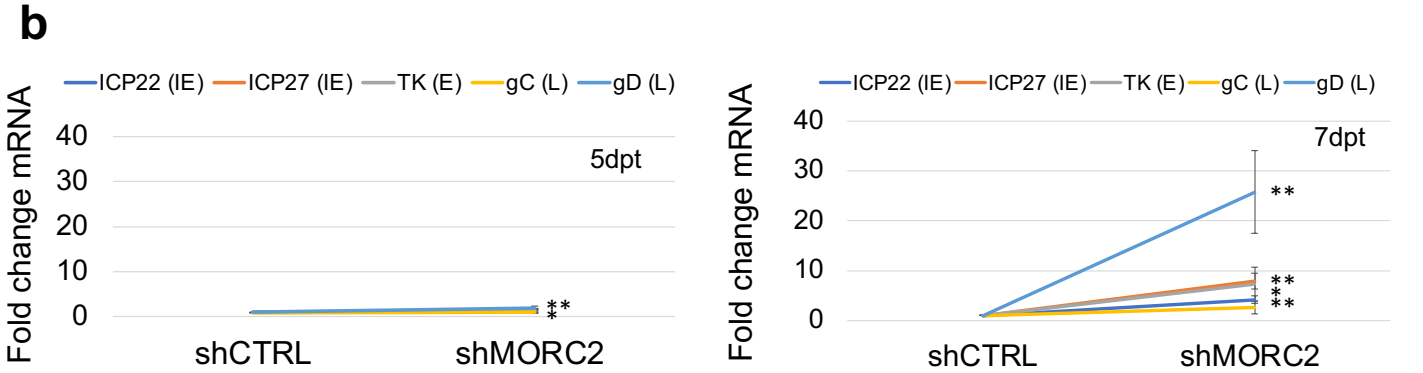
b
ICP22 (IE)
ICP27 (IE)
TK (E)
gC (L)
gD (L)
Fold change mRNA
5dpt
7dpt
shCTRL
shMORC2
**

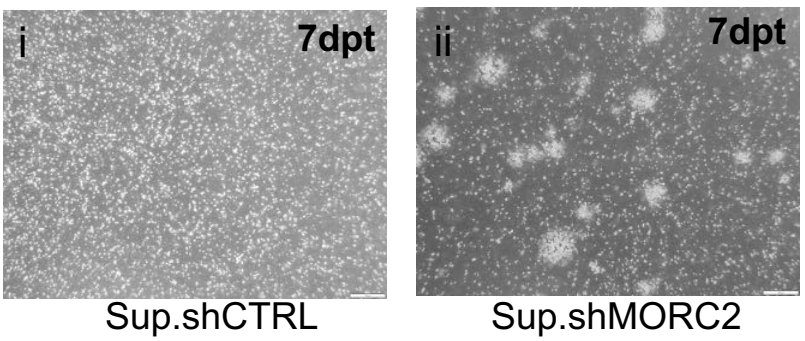
c
i
ii
7dpt
Sup.shCTRL
Sup.shMORC2

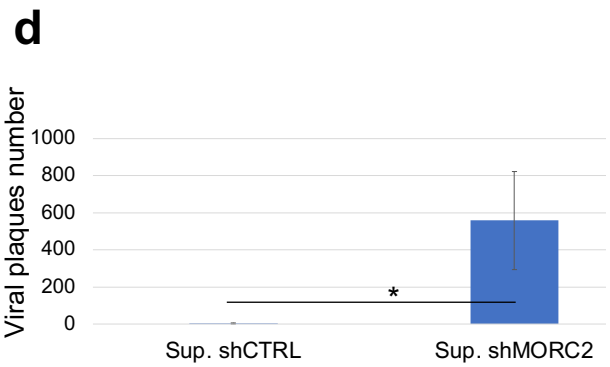
d
Viral plaques number
Sup. shCTRL
Sup. shMORC2
*

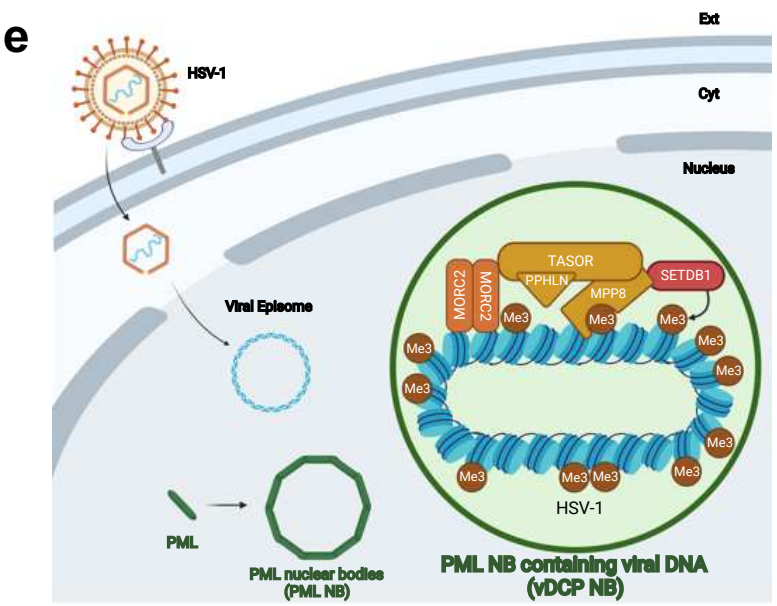
e
HSV-1
Ext
Cyt
Nucleus
Viral Episome
TASOR
PPHLN
MPP8
SETDB1
MORC2
Me3
PML
PML nuclear bodies (PML NB)
PML NB containing viral DNA (vDCP NB)

Figure S1

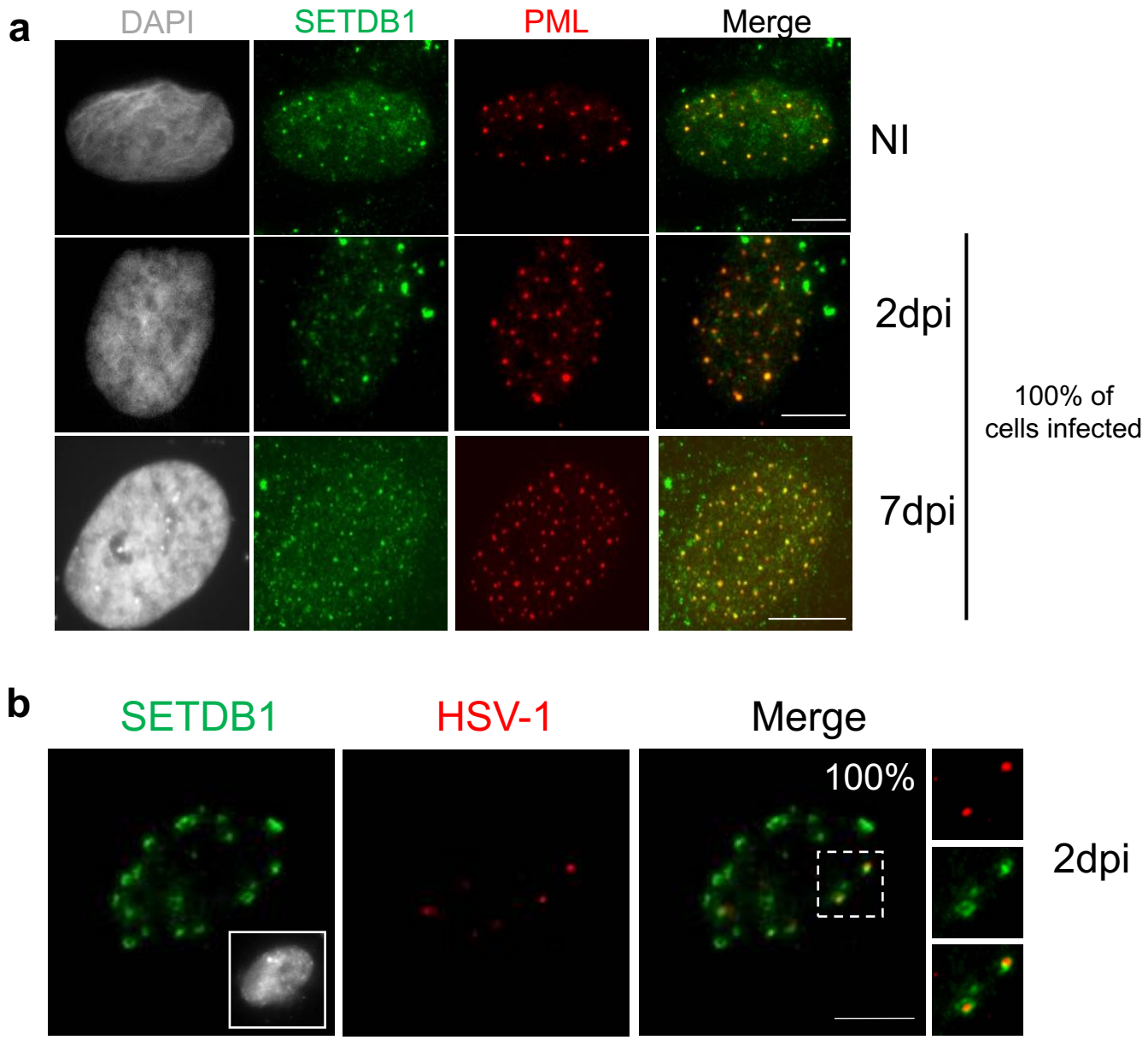
a
DAPI
SETDB1
PML
Merge
NI
2dpi
7dpi
100% of cells infected
b
SETDB1
HSV-1
Merge
100%
2dpi

Figure S2

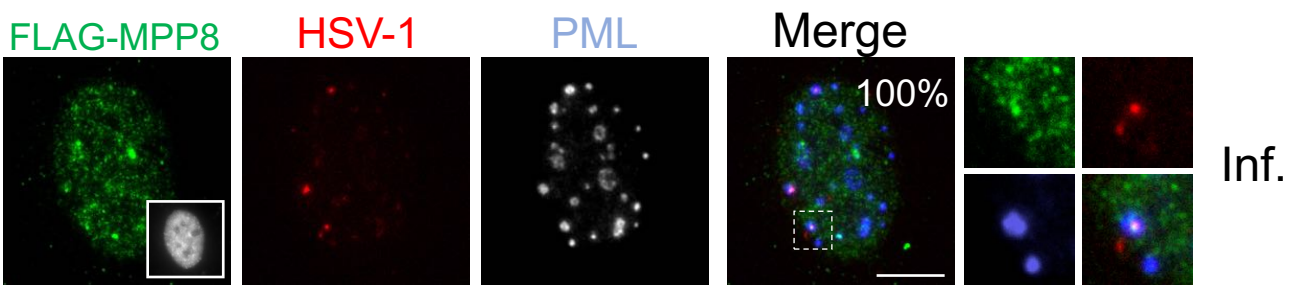

Figure S3

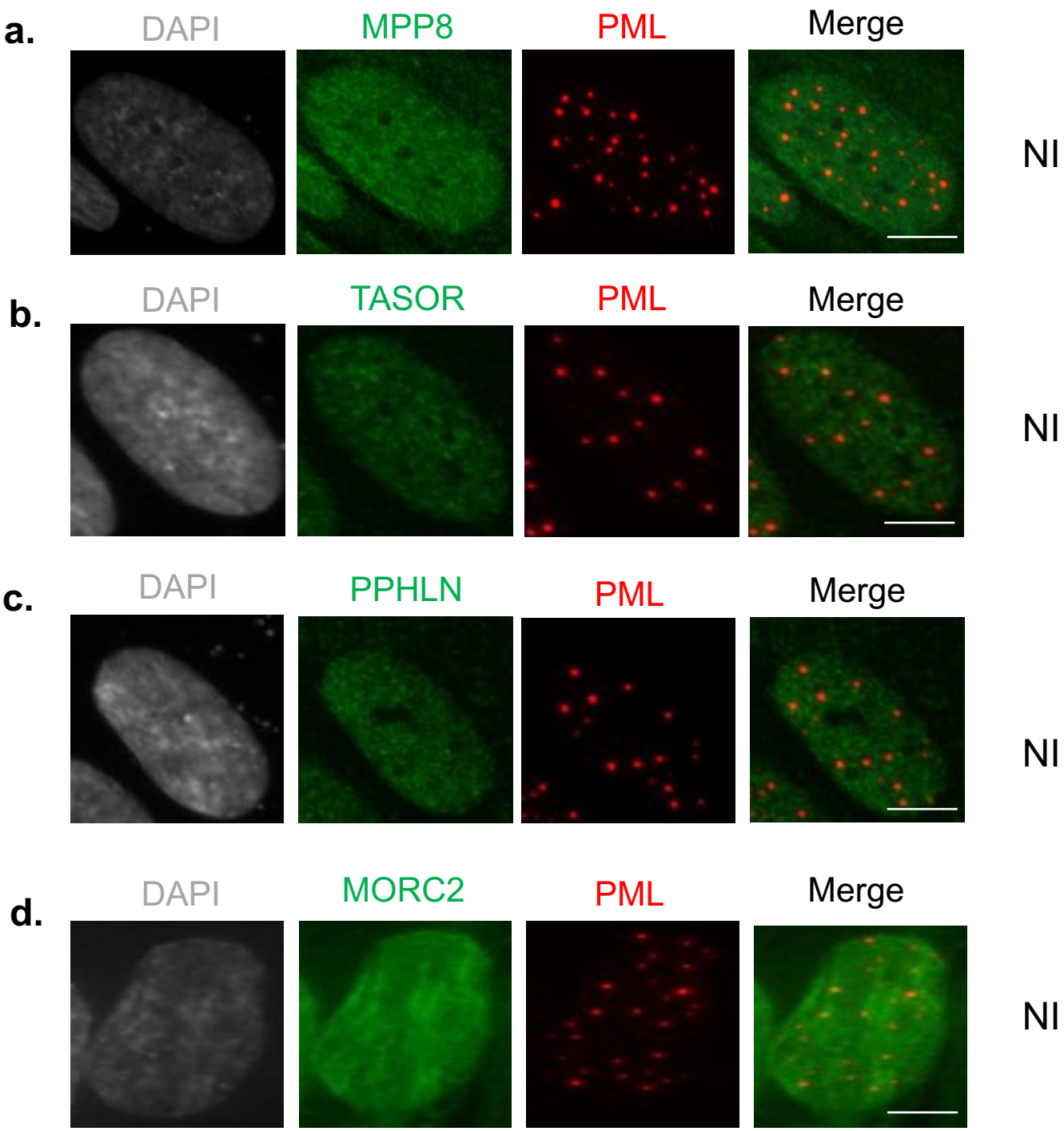
a.
DAPI
MPP8
PML
Merge
NI
b.
DAPI
TASOR
PML
Merge
NI
c.
DAPI
PPHLN
PML
Merge
NI
d.
DAPI
MORC2
PML
Merge
NI

Figure S4

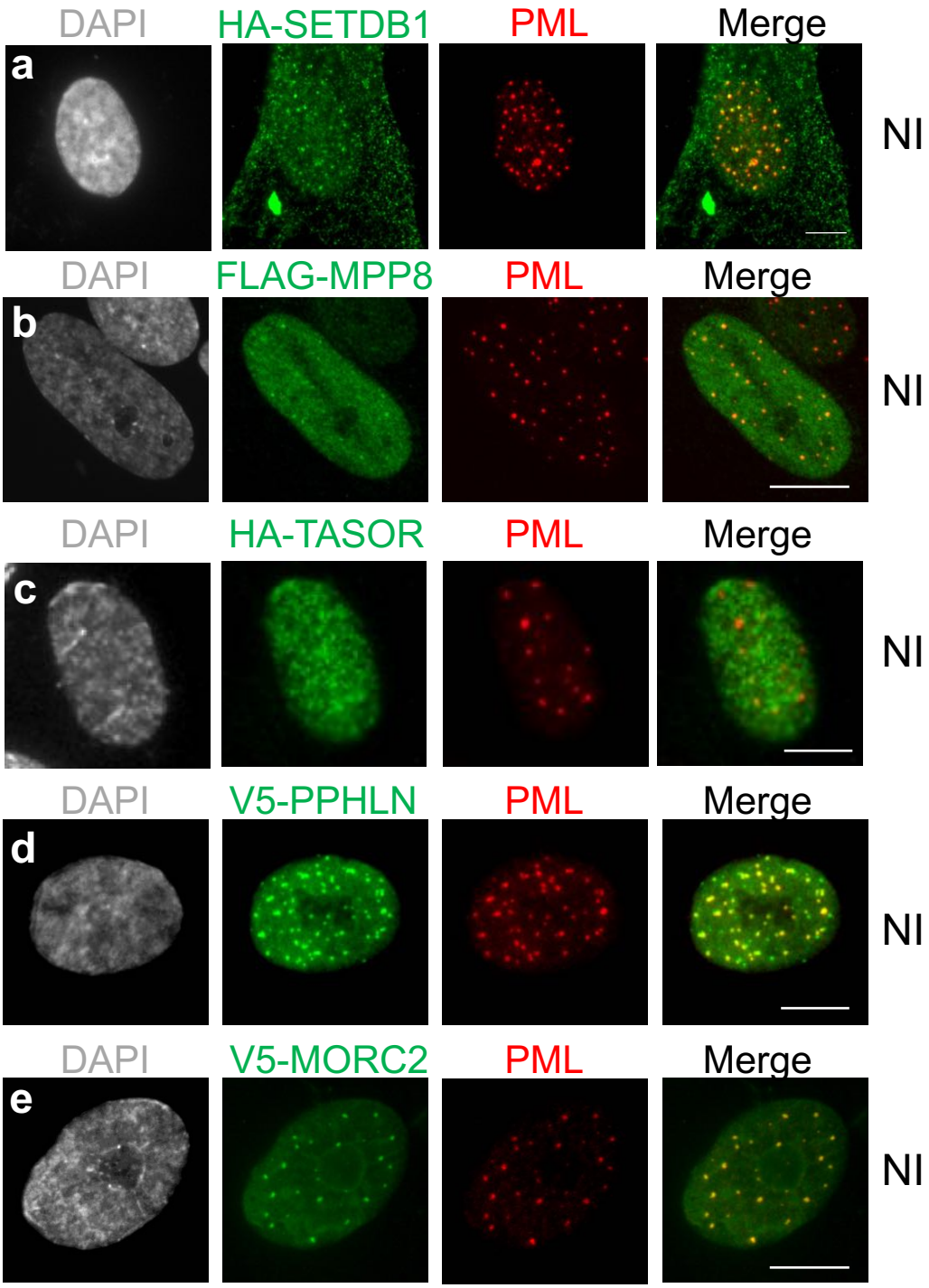
DAPI
HA-SETDB1
PML
Merge
a
NI
DAPI
FLAG-MPP8
PML
Merge
b
NI
DAPI
HA-TASOR
PML
Merge
c
NI
DAPI
V5-PPHLN
PML
Merge
d
NI
DAPI
V5-MORC2
PML
Merge
e
NI

Figure S5

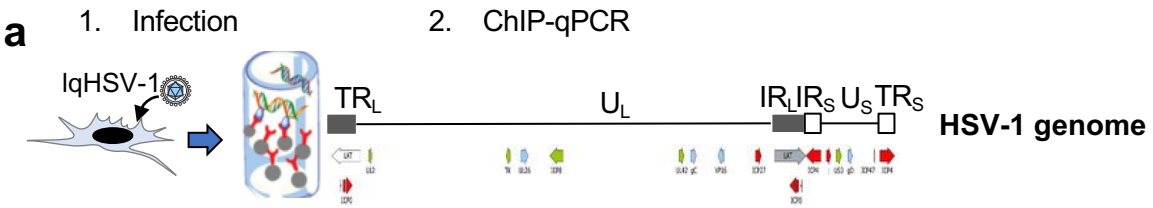
a
1. Infection
2. ChIP-qPCR
lqHSV-1
TRL
UL
IRLIRS US TRS
HSV-1 genome

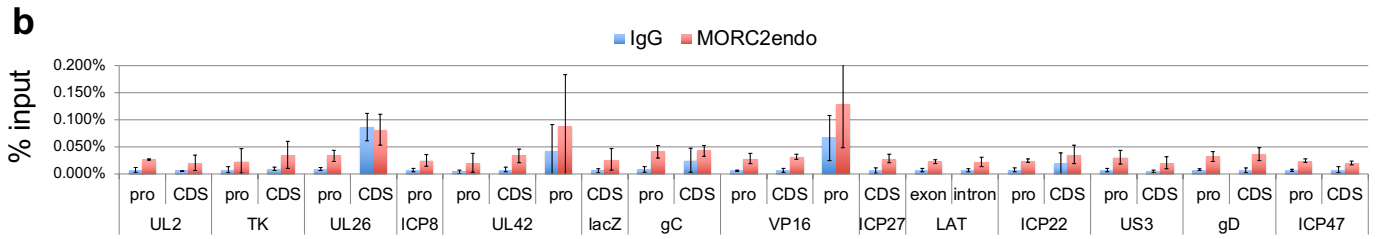
b
IgG
MORC2endo
% input
0.200%
0.150%
0.100%
0.050%
0.000%
pro CDS pro CDS pro CDS pro pro CDS pro CDS pro CDS pro CDS pro CDS exon intron pro CDS pro CDS pro CDS pro CDS
UL2 TK UL26 ICP8 UL42 lacZ gC VP16 ICP27 LAT ICP22 US3 gD ICP47

Figure S6

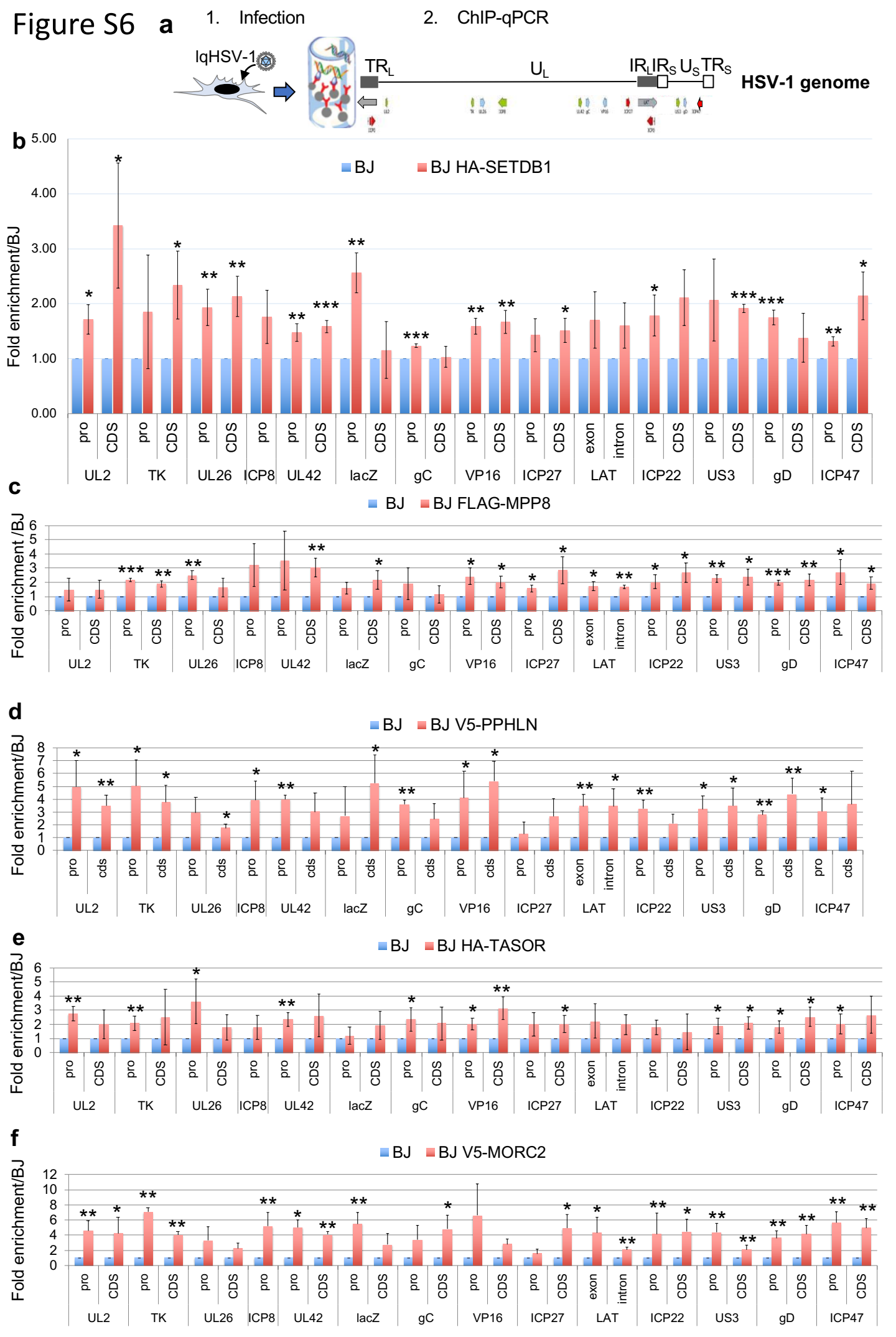
a
1. Infection
2. ChIP-qPCR
lqHSV-1
TRL
UL
IRLIRS US TRS
HSV-1 genome
b
BJ
BJ HA-SETDB1
Fold enrichment/BJ
c
BJ
BJ FLAG-MPP8
Fold enrichment /BJ
d
BJ
BJ V5-PPHLN
Fold enrichment/BJ
e
BJ
BJ HA-TASOR
Fold enrichment/BJ
f
BJ
BJ V5-MORC2
Fold enrichment/BJ
pro
CDS
cds
exon
intron
UL2
TK
UL26
ICP8
UL42
lacZ
gC
VP16
ICP27
LAT
ICP22
US3
gD
ICP47

Figure S7

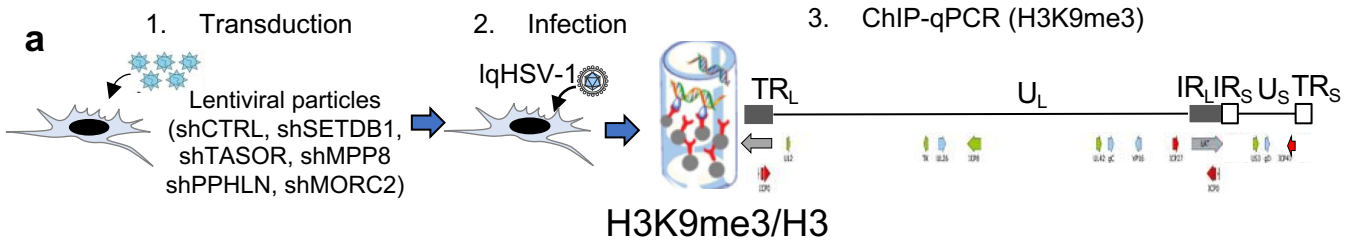
a
1. Transduction
2. Infection
3. ChIP-qPCR (H3K9me3)
Lentiviral particles
(shCTRL, shSETDB1,
shTASOR, shMPP8
shPPHLN, shMORC2)
lqHSV-1
TRL
UL
IRL IRS US TRS
H3K9me3/H3

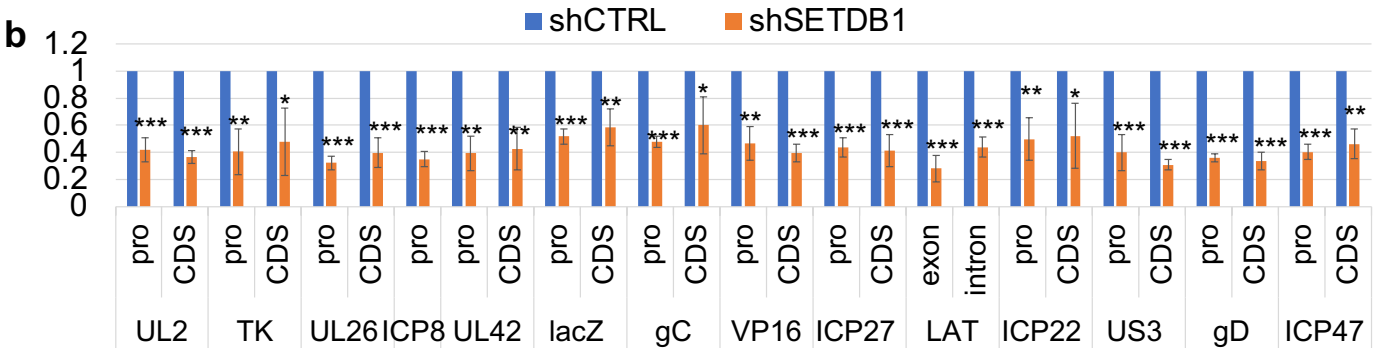
b
shCTRL
shSETDB1
1.2
1
0.8
0.6
0.4
0.2
0
pro
CDS
exon
intron
UL2
TK
UL26
ICP8
UL42
lacZ
gC
VP16
ICP27
LAT
ICP22
US3
gD
ICP47

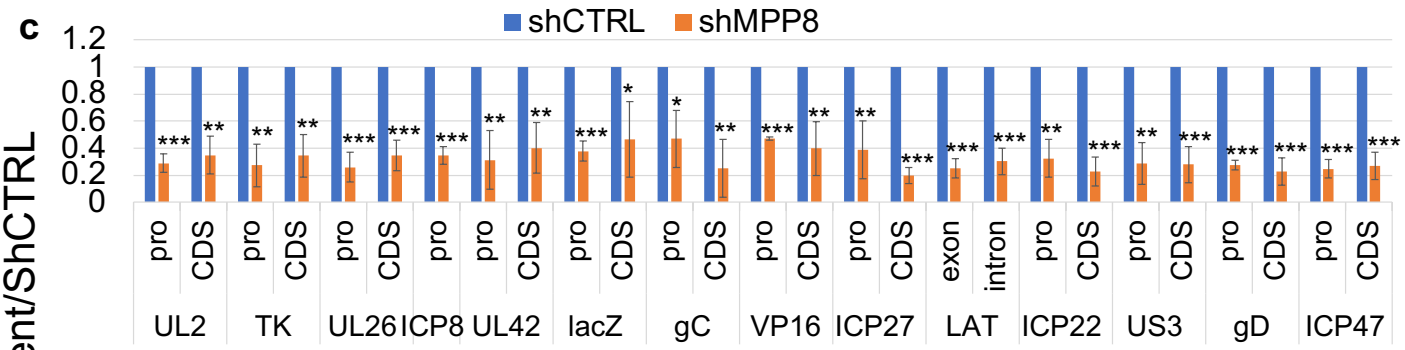
c
shCTRL
shMPP8
Fold enrichment/ShCTRL
1.2
1
0.8
0.6
0.4
0.2
0
pro
CDS
exon
intron
UL2
TK
UL26
ICP8
UL42
lacZ
gC
VP16
ICP27
LAT
ICP22
US3
gD
ICP47

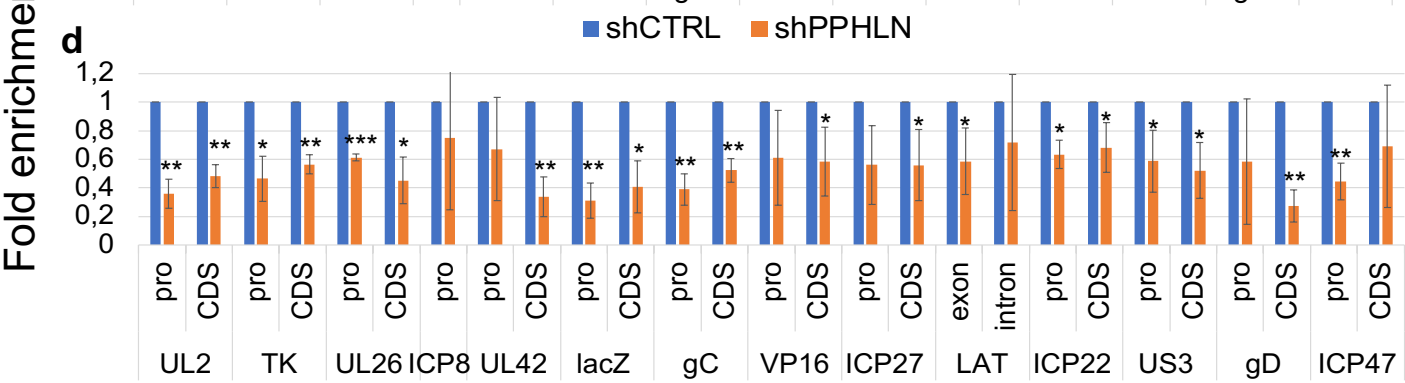
d
shCTRL
shPPHLN
1,2
1
0,8
0,6
0,4
0,2
0
pro
CDS
exon
intron
UL2
TK
UL26
ICP8
UL42
lacZ
gC
VP16
ICP27
LAT
ICP22
US3
gD
ICP47

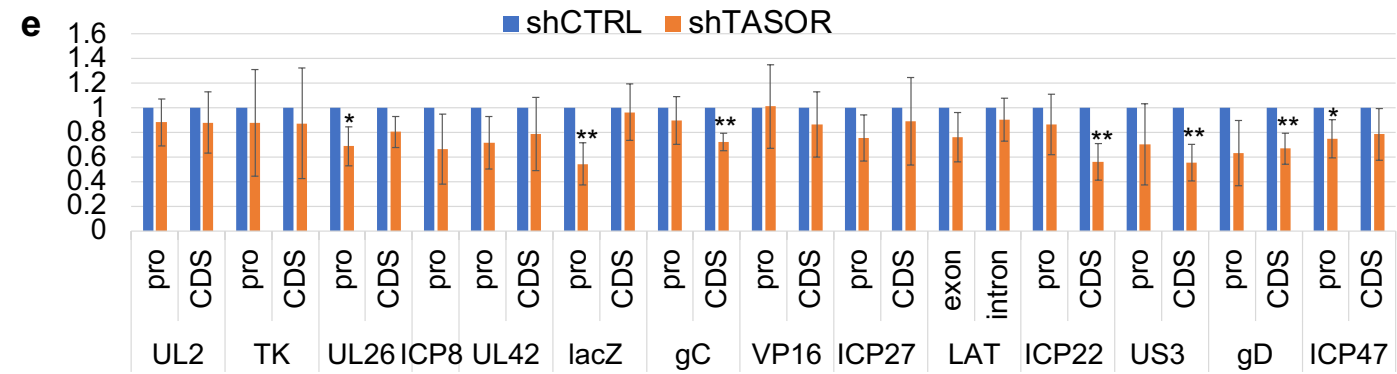
e
shCTRL
shTASOR
1.6
1.4
1.2
1
0.8
0.6
0.4
0.2
0
pro
CDS
exon
intron
UL2
TK
UL26
ICP8
UL42
lacZ
gC
VP16
ICP27
LAT
ICP22
US3
gD
ICP47

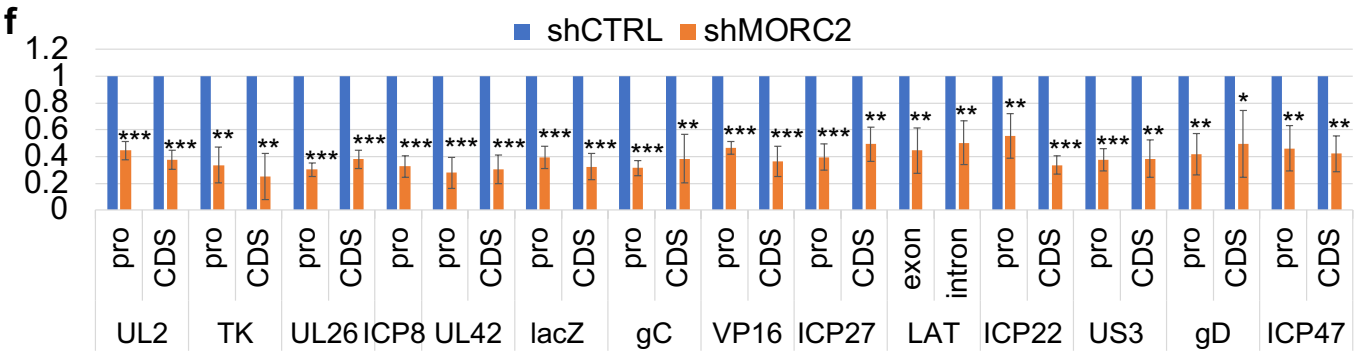
f
shCTRL
shMORC2
1.2
1
0.8
0.6
0.4
0.2
0
pro
CDS
exon
intron
UL2
TK
UL26
ICP8
UL42
lacZ
gC
VP16
ICP27
LAT
ICP22
US3
gD
ICP47

Figure S8

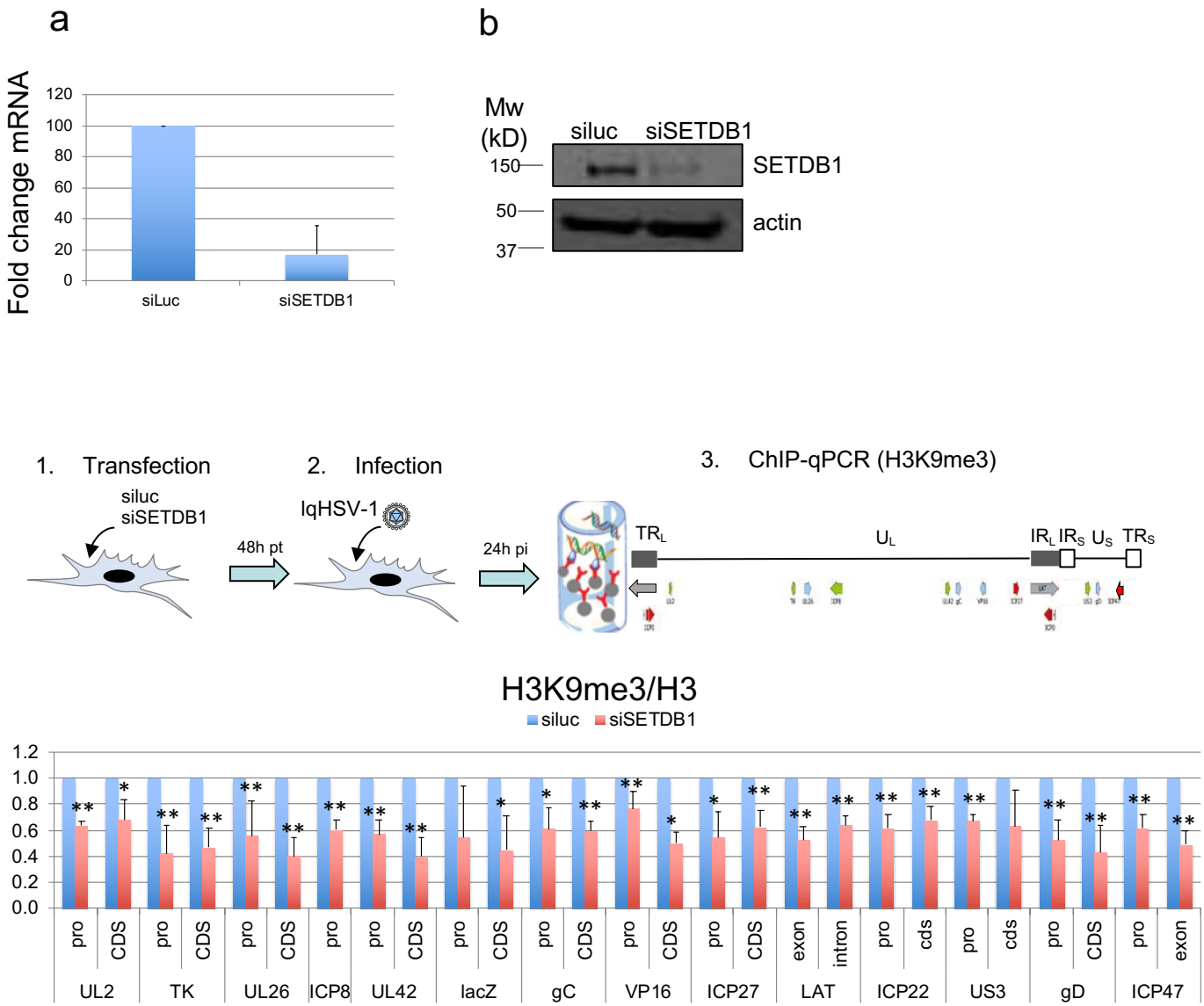
a
Fold change mRNA
120
100
80
60
40
20
0
siLuc
siSETDB1
b
Mw
(kD)
siluc
siSETDB1
150
50
37
SETDB1
actin
c
1. Transfection
siluc
siSETDB1
48h pt
2. Infection
lqHSV-1
24h pi
3. ChIP-qPCR (H3K9me3)
TRL
UL
IRL IRS US TRS
d
H3K9me3/H3
siluc
siSETDB1
Fold enrichment/Siluc
1.2
1.0
0.8
0.6
0.4
0.2
0.0
pro
CDS
UL2
TK
UL26
ICP8
UL42
lacZ
gC
VP16
ICP27
exon
intron
LAT
cds
ICP22
US3
gD
ICP47

Figure S9

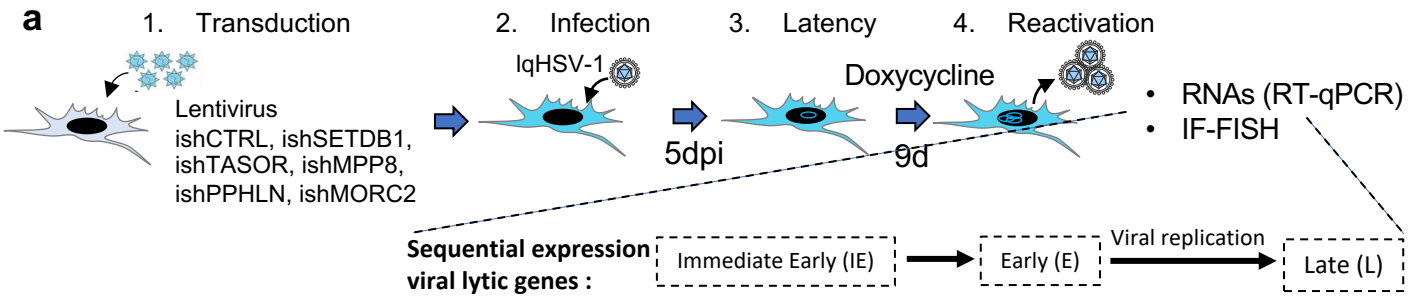
a
1. Transduction
2. Infection
3. Latency
4. Reactivation
Lentivirus
ishCTRL, ishSETDB1,
ishTASOR, ishMPP8,
ishPPHLN, ishMORC2
lqHSV-1
5dpi
Doxycycline
9d
• RNAs (RT-qPCR)
• IF-FISH
Sequential expression
viral lytic genes :
Immediate Early (IE)
Early (E)
Viral replication
Late (L)

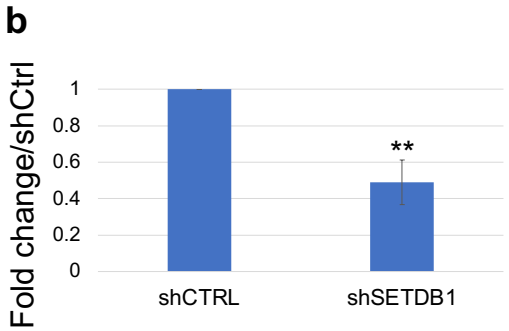
b
Fold change/shCtrl
1
0.8
0.6
0.4
0.2
0
**
shCTRL
shSETDB1

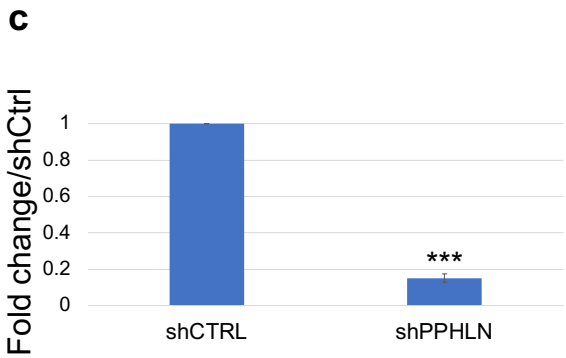
c
Fold change/shCtrl
1
0.8
0.6
0.4
0.2
0
***
shCTRL
shPPHLN

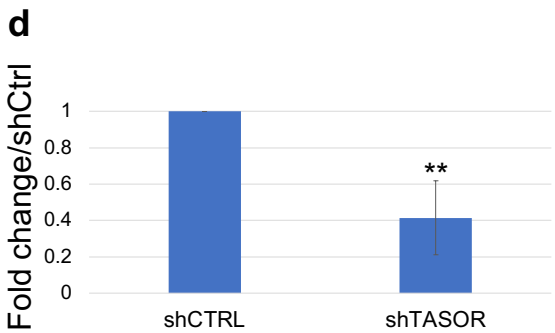
d
Fold change/shCtrl
1
0.8
0.6
0.4
0.2
0
**
shCTRL
shTASOR

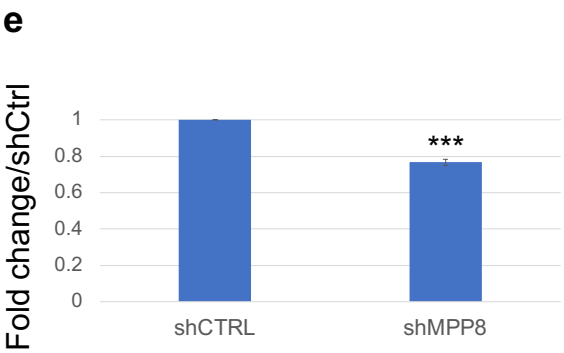
e
Fold change/shCtrl
1
0.8
0.6
0.4
0.2
0
***
shCTRL
shMPP8

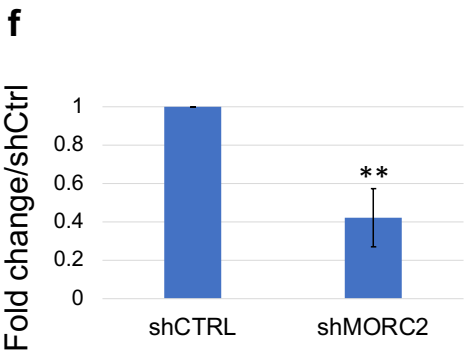
f
Fold change/shCtrl
1
0.8
0.6
0.4
0.2
0
**
shCTRL
shMORC2

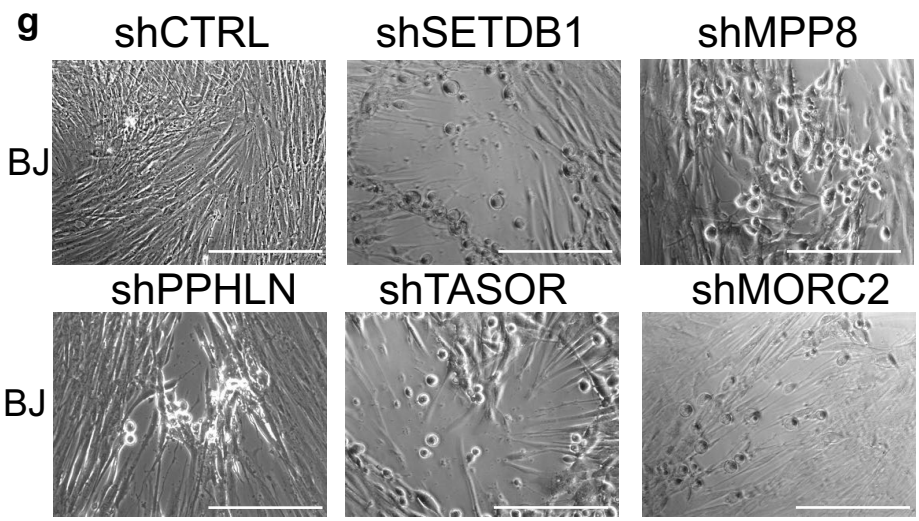
g
shCTRL
shSETDB1
shMPP8
BJ
shPPHLN
shTASOR
shMORC2
BJ

Figure S10

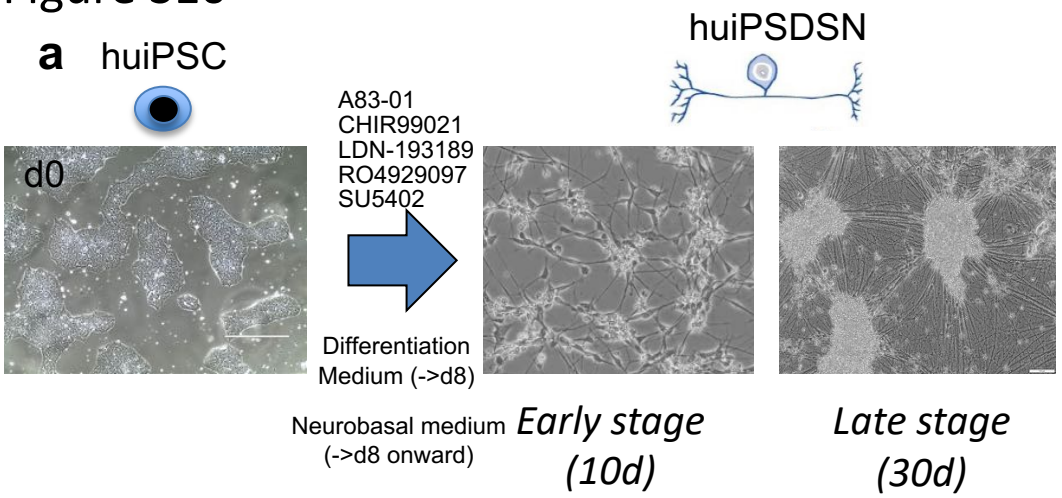
a
huiPSC
huiPSDSN
d0
A83-01
CHIR99021
LDN-193189
RO4929097
SU5402
Differentiation Medium (->d8)
Neurobasal medium (->d8 onward)
Early stage (10d)
Late stage (30d)

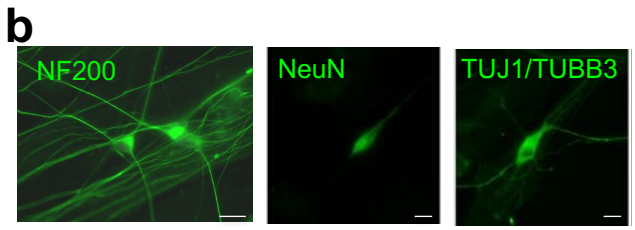
b
NF200
NeuN
TUJ1/TUBB3

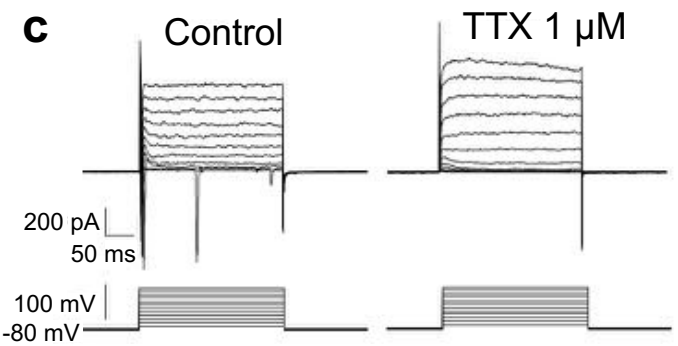
c
Control
TTX 1 μM
200 pA
50 ms
100 mV
-80 mV

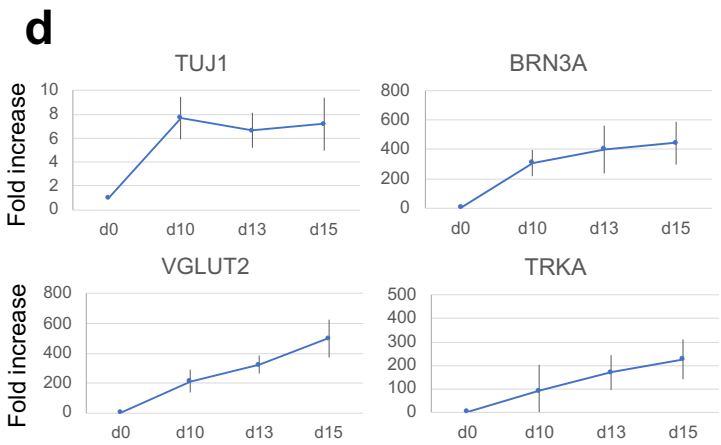
d
TUJ1
BRN3A
VGLUT2
TRKA
Fold increase
d0
d10
d13
d15

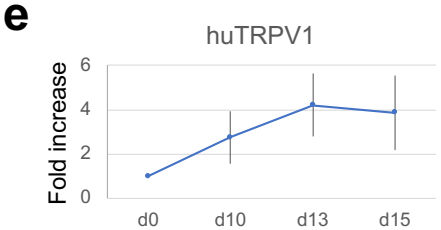
e
huTRPV1
Fold increase
d0
d10
d13
d15

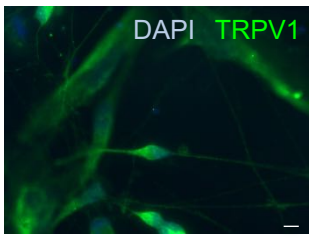
f
DAPI TRPV1

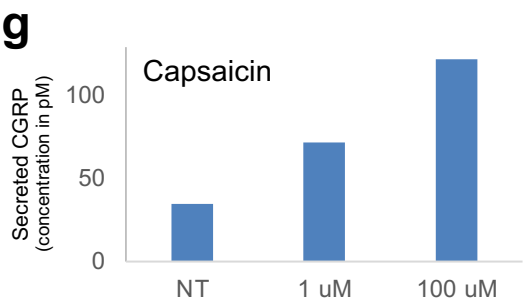
g
Capsaicin
Secreted CGRP (concentration in pM)
NT
1 uM
100 uM

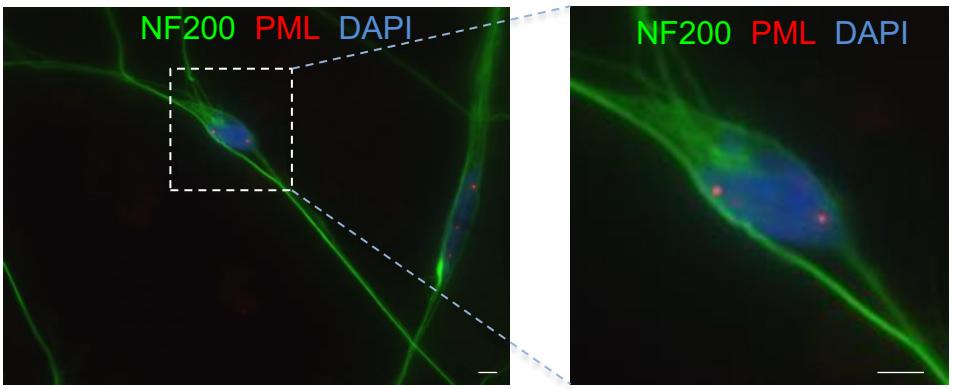
h
NF200 PML DAPI
NF200 PML DAPI

Figure S11

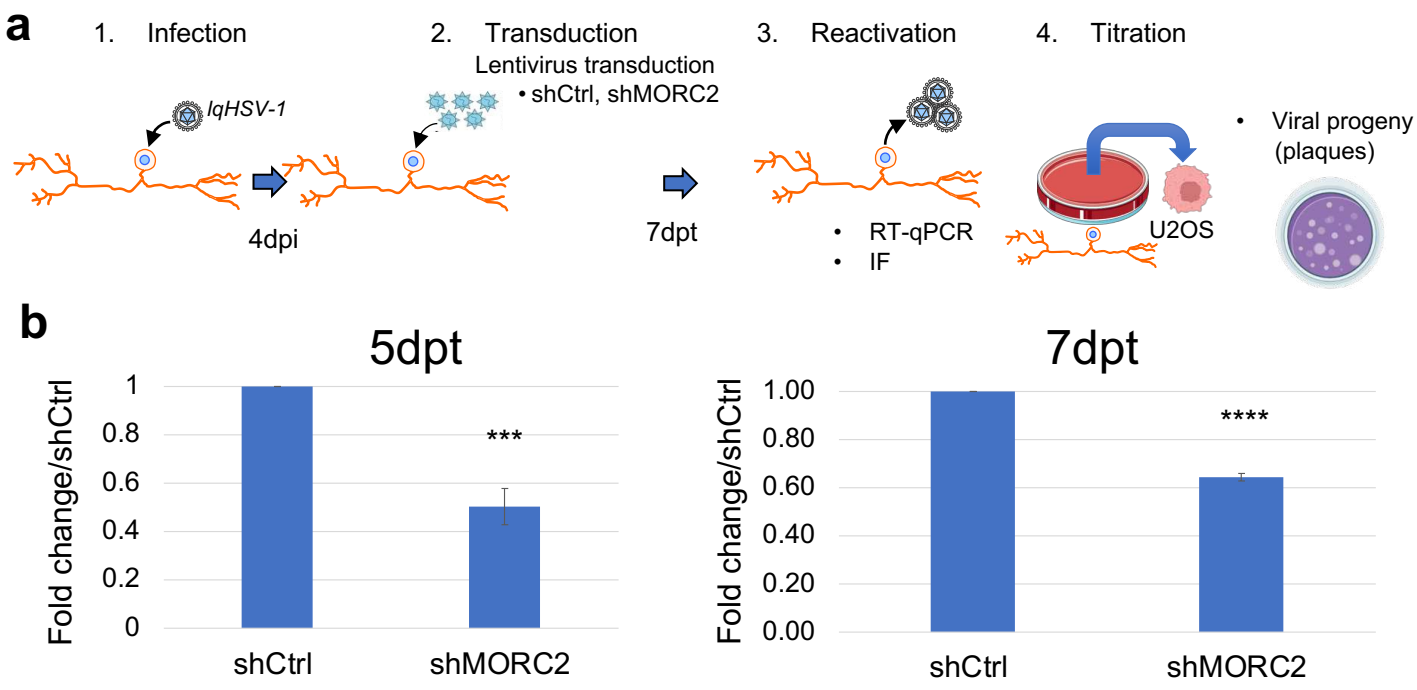
a
1. Infection
2. Transduction
Lentivirus transduction
• shCtrl, shMORC2
3. Reactivation
4. Titration
lqHSV-1
4dpi
7dpt
• RT-qPCR
• IF
U2OS
• Viral progeny (plaques)

b
5dpt
Fold change/shCtrl
1
0.8
0.6
0.4
0.2
0
***
shCtrl
shMORC2
7dpt
Fold change/shCtrl
1.00
0.80
0.60
0.40
0.20
0.00
****
shCtrl
shMORC2